

CENTRALIZED TRAINING WITH HYBRID EXECUTION IN MULTI-AGENT REINFORCEMENT LEARNING

**Pedro P. Santos*, Diogo S. Carvalho*, Miguel Vasco*,
Alberto Sardinha, Pedro A. Santos, Ana Paiva & Francisco S. Melo**
INESC-ID & Instituto Superior Técnico, University of Lisbon
{pedro.pinto.santos, diogo.s.carvalho,
miguel.vasco}@tecnico.ulisboa.pt

ABSTRACT

We introduce *hybrid* execution in multi-agent reinforcement learning (MARL), a new paradigm in which agents aim to successfully perform cooperative tasks with any communication level at execution time by taking advantage of information-sharing among the agents. Under hybrid execution, the communication level can range from a setting in which no communication is allowed between agents (fully decentralized), to a setting featuring full communication (fully centralized). To formalize our setting, we define a new class of multi-agent partially observable Markov decision processes (POMDPs) that we name hybrid-POMDPs, which explicitly models a communication process between the agents. We contribute MARO, an approach that combines an autoregressive predictive model to estimate missing agents’ observations, and a dropout-based RL training scheme that simulates different communication levels during the centralized training phase. We evaluate MARO on standard scenarios and extensions of previous benchmarks tailored to emphasize the negative impact of partial observability in MARL. Experimental results show that our method consistently outperforms baselines, allowing agents to act with faulty communication while successfully exploiting shared information.

1 INTRODUCTION

Multi-agent reinforcement learning (MARL) aims to learn utility-maximizing behavior in scenarios involving multiple agents. In recent years, deep MARL methods have been successfully applied to multi-agent tasks such as game-playing (Papoudakis et al., 2020), traffic light control (Wei et al., 2019), or energy management (Fang et al., 2020). Despite recent successes, the multi-agent setting happens to be substantially harder than its single-agent counterpart (Canese et al., 2021) because multiple concurrent learners can create non-stationarity conditions that hinder learning; the curse of dimensionality obstructs centralized approaches to MARL due to the exponential growth in state and action spaces with the number of agents; and agents seldom observe the true state of the environment.

As a way to deal with the exponential growth in the state/action space and with environmental constraints, both in perception and actuation, existing methods aim to learn decentralized policies that allow the agents to act based on local perceptions and partial information about other agents’ intentions. The paradigm of *centralized training with decentralized execution* is undoubtedly at the core of recent research in the field (Oliehoek et al., 2011; Rashid et al., 2018; Foerster et al., 2016); such paradigm takes advantage of the fact that additional information, available only at training time, can be used to learn decentralized policies in a way that the need for communication is alleviated.

While in some settings partial observability and/or communication constraints require learning fully decentralized policies, the assumption that agents cannot communicate at execution time is often too restrictive for a great number of real-world application domains such as robotics, game-playing or autonomous driving (Ho et al., 2019; Yurtsever et al., 2020). In such domains, learning fully decentralized policies should be deemed inappropriate since such policies do not take into account the possibility of communication between the agents. Other MARL strategies, which take advantage of additional information shared among the agents, can surely be developed (Zhu et al., 2022).

*Equal contribution.

In this work, our objective is to develop agents that are able to exploit the benefits of centralized training while, simultaneously, taking advantage of information-sharing at execution time. We introduce the paradigm of *hybrid* execution, in which agents act in scenarios with any possible communication level, ranging from no communication (fully decentralized) to full communication between the agents (fully centralized). In particular, we consider scenarios with faulty communication during execution, in which agents passively share their local observations and actions to perform partially observable cooperative tasks. To formalize our setting, we start by defining *hybrid partially observable Markov decision process* (H-POMDP), a new class of multi-agent POMDPs that explicitly considers a communication process between the agents. Our goal is to find a method that allows agents to solve H-POMDPs regardless of the communication process encountered at execution time. To allow for hybrid execution, we propose an autoregressive model that explicitly predicts non-shared information from past observations of the agents. In addition, we propose a training scheme for the agents’ controllers that simulates communication faults during the centralized training phase. We denote our coupled approach by *multi-agent observation sharing with communication dropout* (MARO). MARO can be easily integrated with current deep MARL methods.

We evaluate the performance of MARO across different communication levels, in different MARL benchmark environments and using multiple RL algorithms. Furthermore, we introduce three novel MARL environments that explicitly require communication during execution to successfully perform cooperative tasks, currently missing in literature. Finally, we perform an ablation study that highlights the importance of both the predictive model and the training scheme to the overall performance of MARO. The results show that our method consistently outperforms the baselines, allowing agents to exploit shared information during execution and perform tasks under various communication levels.

In summary, our contribution is three-fold: (i) we propose and formalize the setting of hybrid execution in MARL, in which agents must perform partially-observable cooperative tasks across all possible communication levels; (ii) we propose MARO, an approach that combines an autoregressive predictive model of agents’ observations and a novel training scheme; and (iii) we evaluate MARO in different benchmark and novel environments, using different RL algorithms, showing that our approach consistently allows agents to act with different communication levels.

2 HYBRID EXECUTION IN MULTI-AGENT REINFORCEMENT LEARNING

A fully cooperative multi-agent system with Markovian dynamics can be modelled as a decentralized partially observable Markov decision process (Dec-POMDP) (Oliehoek & Amato, 2016). A Dec-POMDP is a tuple $([n], \mathcal{X}, \mathcal{A}, \mathcal{P}, r, \gamma, \mathcal{Z}, \mathcal{O})$, where $[n] = \{1, \dots, n\}$ is the set of indexes of n agents, \mathcal{X} is the set of states of the environment, $\mathcal{A} = \times_i \mathcal{A}_i$ is the set of joint actions, where \mathcal{A}_i is the set of individual actions of agent i , \mathcal{P} is the set of probability distributions over next states in \mathcal{X} , one for each state and action in $\mathcal{X} \times \mathcal{A}$, $r : \mathcal{X} \times \mathcal{A} \rightarrow \mathbb{R}$ maps states and actions to expected rewards, $\gamma \in [0, 1[$ is a discount factor, $\mathcal{Z} = \times_i \mathcal{Z}_i$ is the set of joint observations, where \mathcal{Z}_i is the set of local observations of agent i , and \mathcal{O} is the set of probability distributions over joint observations in \mathcal{Z} , one for each state and action in $\mathcal{X} \times \mathcal{A}$. A decentralized policy for agent i is $\pi_i : \mathcal{Z}_i \rightarrow \mathcal{A}_i$ and the joint decentralized policy is $\pi : \mathcal{Z} \rightarrow \mathcal{A}$ such that $\pi(z_1, \dots, z_n) = (\pi_1(z_1), \dots, \pi_n(z_n))$. Fully decentralized approaches to MARL directly apply standard single-agent RL algorithms for learning each agents’ policy π_i in a decentralized manner. In Independent Q -learning (IQL) (Tan, 1993), each agent treats other agents as being part of the environment, ignoring influences of other agents’ observations and actions. More recently, under the paradigm of centralized training with decentralized execution, QMIX (Rashid et al., 2018) aims at learning decentralized policies with centralization at training time while fostering cooperation among the agents. Finally, if we know that all agents can share their local observations among themselves at execution time, we can use either of the two approaches to learn fully centralized policies.

None of the classes of methods aforementioned assumes that agents may sometimes have access to other agents’ observations and sometimes not. Therefore, decentralized agents are unable to take advantage of the additional information that they may receive from other agents at execution time, and centralized agents are unable to act when the sharing of information fails. In this work, we introduce hybrid execution in MARL, a setting in which agents act regardless of the communication process while taking advantage of additional information they may receive during execution. To

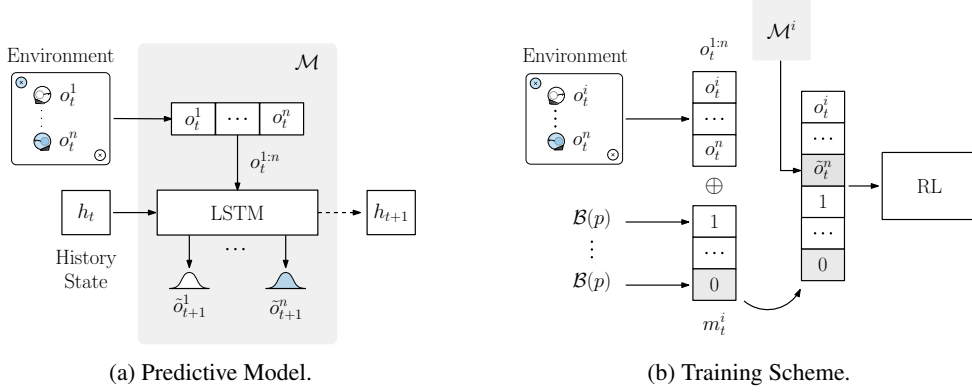


Figure 1: Our proposed MARO approach for hybrid execution: (a) we introduced an autoregressive predictive model \mathcal{M} to estimate the next-step observations $p(o_{t+1}^{1:n} | o_t^{1:n}, h_t)$ from the previous ones $o_t^{1:n}$ and an history variable h_t ; (b) we introduce a training scheme for RL controllers that randomly drops agent observations following the communication masks m_t^i , sampled accordingly to the communication level p . More details in the main text.

formalize this setting, we define a new class of multi-agent POMDPs that we name hybrid-POMDPs (H-POMDPs), which explicitly considers a specific communication process among the agents.

2.1 HYBRID PARTIALLY OBSERVABLE MARKOV DECISION PROCESSES

We define an hybrid-POMDP (H-POMDP) as a tuple $([n], \mathcal{X}, \mathcal{A}, \mathcal{P}, r, \gamma, \mathcal{Z}, \mathcal{O}, C)$ where, in addition to the tuple that describes the Dec-POMDP, we consider an $n \times n$ communication matrix C such that $[C]_{i,j} = p_{i,j}$ is the probability that, at a certain time step, agent i has access to the local observation of agent j in \mathcal{Z}_j . H-POMDPs generalize both the notion of decentralized execution and of centralized execution in MARL. Specifically, for a given Dec-POMDP, we can consider C the identity matrix to capture fully decentralized execution and C a matrix of ones to capture fully centralized execution.

In our setting, we assume that at execution time agents will face an H-POMDP with an unknown communication matrix C , sampled from a set \mathcal{C} according to an unknown probability distribution μ . The performance of the agent is measured as $J_\mu(\pi) = \mathbb{E}_{C \sim \mu} [J(\pi; C)]$, where $J(\pi; C)$ denotes the expected discounted cumulative reward under an H-POMDP with communication matrix C . At training time, agents may have access to the fully centralized H-POMDP. Therefore, the setting we consider is one of centralized training with hybrid execution and unknown communication process.

We note here that every H-POMDP has a corresponding Dec-POMDP, which can be obtained by adequately changing the observation space \mathcal{Z} and the set of emission probability distributions \mathcal{O} . Consequently, any reinforcement learning method can be trained to solve a specific H-POMDP, with a specific communication matrix C , by solving the corresponding Dec-POMDP. However, we seek to find a method that takes explicit advantage of the characteristics of hybrid execution to be able to act on H-POMDPs regardless of the matrix C that models the communication process at execution time. To the best of our knowledge, there exists no documentation of a method that solves our problem.

3 MULTI-AGENT OBSERVATION SHARING WITH COMMUNICATION DROPOUT

While acting on an H-POMDP, agents may not have access to all perceptual information due to a faulty communication process. We propose MARO, a novel approach to exploit shared information and overcome communication issues during task execution. MARO is composed of two elements: an autoregressive predictive model that estimates missing information from previous observations, and a training scheme for the RL controllers that simulates faulty communication at training time.

3.1 PREDICTIVE MODEL

The predictive model \mathcal{M} , depicted in Fig. 1a, is used to estimate the local observations of all agents $o_t^{1:n} = \{o_t^1, \dots, o_t^n\}$, where o_t^i corresponds to the observation of the i -th agent, in order to overcome missing observations during execution. Thus, we learn a transition model $p(o_{t+1}^{1:n} | o_t^{1:n}, h_t)$ that given the current observations $o_t^{1:n}$ and some history variable h_t , containing information regarding the policy of the agents, is able to predict the next-step observations o_{t+1} . We instantiate $p_\theta(o_{t+1}^{1:n} | o_t^{1:n}, h_t)$ as an LSTM, parameterized by θ , with:

$$p_\theta(o_{t+1}^{1:n} | o_t^{1:n}, h_t) = \prod_{i=1}^n p_\theta(o_{t+1}^i | o_t^{1:n}, h_t), \quad (1)$$

where $p_\theta(o_{t+1}^i | o_t^{1:n}, h_t)$ is the Gaussian distribution of the predicted observations of the i -th agent. We train the predictive model and RL controllers simultaneously: we consider single-step observation transitions $(o_t^{1:n}, o_{t+1}^{1:n})$ and evaluate the negative log-likelihood of the target next-step observation $o_{t+1}^{1:n}$, given the estimated next-step observation distribution $p_\theta(\cdot | o_t^{1:n}, h_t)$:

$$\mathcal{L}_{\mathcal{M}}(o_t^{1:n}, o_{t+1}^{1:n}) = - \sum_{i=1}^n \log p_\theta(o_{t+1}^i | o_t^{1:n}, h_t). \quad (2)$$

3.2 TRAINING SCHEME

We also introduce an RL training scheme, depicted in Fig. 1b, which simulates the communication process at execution time and is agnostic to the type of algorithm. We setup all RL controllers to receive as input the joint observation $o_t^{1:n}$. However, in our setting, some observations may not be shared at execution time. To overcome such issue, we employ the predictive model to estimate the non-shared observations \tilde{o}_t^j , with $j \in [n]$. We also setup the controllers to additionally receive as input *communication masks* m_t , binary vectors that indicate the real and predicted components of $o_t^{1:n}$. These masks implicitly provide the controllers with information regarding the communication level in the environment, enabling them to measure uncertainty regarding the input.

During centralized training, methods typically assume that each agent has access to the local observations of all other agents. Instead of using such information to train the agents, we instead propose to explicitly simulate the communication conditions of execution time: we randomly *dropout* agent observations. At the beginning of each episode, we sample a communication level $p \sim \mathcal{U}(0, 1)$.¹ Given p , we build at each time-step a communication mask $m_t^i = \{0, 1\}^n$ for each agent $i \in [n]$, with $m_t^i[i] = 1$. We sample the communication masks from independent Bernoulli distributions $m_t^i[j] \sim \mathcal{B}(p)$, for $j \in [n] \setminus i$. At execution time, we extract the observation masks m_t^i directly from the environment, according to the actual faults in communication.

The communication mask indicates which components of the agent-specific joint-observation $o_t^{1:n,i}$ are dropped. Specifically, we use the real observation o_t^k if $m_t^i[k] = 1$ and use the estimated observation \tilde{o}_t^k otherwise. We provide each agent with an independent instance of the predictive model \mathcal{M}^i , which updates the estimated joint-observations in the perspective of the agent $\tilde{o}_t^{1:n,i} = \{\tilde{o}_t^{1,i}, \dots, \tilde{o}_t^{n,i}\}$ and maintains an agent-specific history state h_t^i .

4 EVALUATION

In this section, we evaluate our approach for hybrid execution, answering the following questions: **(i)** What is the performance of MARO in multi-agent cooperative tasks with partial observability, considering unknown levels of communication at execution time?; **(ii)** What is the importance of the training scheme for hybrid execution, considering different dropout schemes?; **(iii)** What is the importance of the predictive model for hybrid execution?

To address **(i)**, we evaluate in Sec. 4.3 our approach against other relevant baselines and considering multiple RL algorithms. The results show that MARO outperforms the baselines, allowing the

¹In the absence of prior information regarding the communication level in the environment, in the training scheme we are sampling communication matrices C such that $p_{i,j} = p_{j,i} = p$ and that $p_{i,i} = 1$.

execution of tasks across multiple communication levels. Regarding (ii), we perform in Sec. 4.4.1 an ablation of the training scheme, highlighting the importance of simulating the communication process at execution time during training. We address (iii) in Sec. 4.4.2, highlighting the benefits of the predictive model, both in terms of training sample efficiency and in allowing centralized execution agents to exploit shared information across multiple communication levels.

4.1 SCENARIOS

We focus our evaluation on multi-agent cooperative environments. As discussed by Papoudakis et al. (2021b), the main challenges in current MARL benchmark scenarios, involve coordination, large action space, sparse reward and non-stationarity. Thus, in order to emphasize the impact of communication, we propose three environments adapted from (Lowe et al., 2017):

- **SpreadXY**: Two heterogeneous agents cover two designated landmarks in a 2D map while avoiding collisions. In this scenario, one of the agents has access to the X-axis position and velocity of both agents, while the other agent has access to the Y-axis position and velocity of both agents. Both agents observe the landmarks’ absolute position;
- **SpreadBlindfold**: Three agents cover three designated landmarks in a 2D map while avoiding collisions. Each agent’s observation only includes its own position and velocity and the absolute position of all landmarks;
- **HearSee**: Two heterogeneous agents cover a single landmark in a 2D map. One of the agents (“Hear” agent) observes the absolute position of the landmark, but it does not have access to its own position in the environment. The other agent (“See” agent) observes the position and velocities of both agents, yet does not have access to the position of the landmark.

In addition to the proposed environments, we evaluate our approach in standard MARL benchmark scenarios, in particular in the SpeakerListener environment. For a complete description of the scenarios, we refer to Appendix B.1.

Finally, we consider H-POMDPs with communication matrices such that each agent i can always access its own local observation, i.e., $p_{i,i} = 1$, and the communication matrix is symmetric between agents i and j , i.e., $p_{i,j} = p_{j,i}$. To simplify the exposition and the evaluation, we use the same $p_{i,j} = p$ for all pairs of different agents i, j . Therefore, we also use p to unambiguously denote the communication level of a given H-POMDP. Additionally, we note that in all the environments the previous action taken by agent i , a_{t-1}^i , is included in its local observation o_t^i .

4.2 BASELINES AND EXPERIMENTAL METHODOLOGY

We compare MARO against different baselines that correspond to different levels of information-sharing between the agents. We consider two “extreme” cases:

- **Observation (Obs.)**: Agents only have access to their own observations and are unable to communicate with other agents, corresponding to standard MARL algorithms designed for decentralized execution;
- **Joint-Observation (J. obs.)**: Agents always have access to the observations of all agents, corresponding to standard MARL algorithms designed for centralized execution. This baseline is unable to perform when communication fails and can be seen as an upper bound.

To the best of our knowledge, there exists no method developed specifically for the problem of executing with faulty communication with unknown dynamics to serve as a direct comparison to MARO. As such, we adapt the model proposed by Kim et al. (2019b) as a baseline:

- **Message-Dropout (MD)**: Agents train with communication failing half of the times (fixed $p = 0.5$), without communication masks and without the predictive model.

We employ the same controller networks across all evaluations. The networks include recurrent layers to mitigate the effects of partial observability. We consider two different MARL algorithms: QMIX and Independent Q -Learning (IQL). We follow the training hyperparameters suggested by

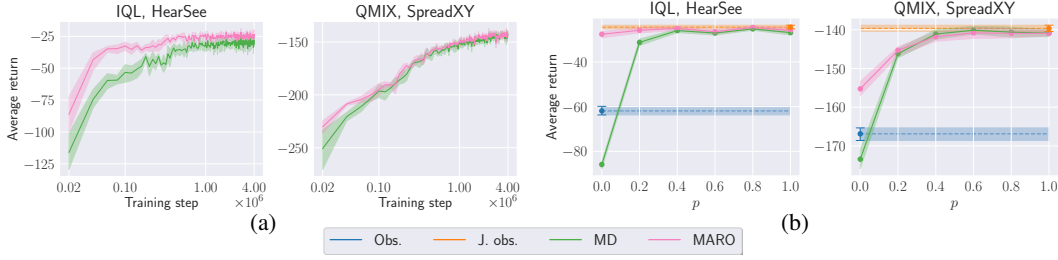


Figure 2: (a) Average episodic returns during training with 95% confidence interval for MARO and MD; (b) Average episodic returns during training with 95% confidence interval for different communication levels at execution time for all approaches. Best viewed with zoom.

Table 1: Average episodic returns and 95% bootstrapped confidence interval over five seeds for all approaches in all scenarios. Higher is better.

Environment	IQL				QMIX			
	Obs.	J. obs.	MD	MARO	Obs.	J. obs.	MD	MARO
SpreadXY	-173.2 (-0.8,+1.1)	-140.3 (-0.8,+0.8)	-150.6 (-1.1,+1.6)	-148.7 (-0.7,+0.7)	-166.9 (-1.7,+1.5)	-139.7 (-0.8,+0.9)	-147.1 (-0.5,+0.5)	-144.2 (-0.5,+0.6)
SpreadBlindfold	-432.2 (-5.9,+6.0)	-403.4 (-5.4,+3.9)	-402.7 (-1.0,+1.0)	-405.3 (-4.3,+3.4)	-418.1 (-3.3,+3.5)	-376.0 (-2.9,+3.3)	-405.7 (-5.0,+5.0)	-401.2 (-6.4,+6.4)
HearSee	-61.9 (-1.8,+2.1)	-24.5 (-0.8,+0.9)	-37.1 (-0.6,+0.6)	-25.9 (-0.3,+0.3)	-54.9 (-1.5,+1.3)	-24.1 (-0.7,+0.9)	-25.4 (-0.4,+0.4)	-25.1 (-0.3,+0.4)
SpeakerListener	-31.7 (-1.2,+1.4)	-25.4 (-1.1,+1.1)	-27.8 (-0.3,+0.3)	-25.6 (-0.5,+0.6)	-26.1 (-1.3,+1.2)	-25.1 (-1.1,+1.1)	-23.2 (-1.0,+1.2)	-23.3 (-1.1,+1.3)

Papoudakis et al. (2021b); we train all models for 4M steps, performing 5 training runs for each experimental setting and 50 evaluation rollouts for each training run. We assume that $p = 1$ at $t = 0$ for the MD and MARO algorithms. The performance of the Obs. and J. Obs. agents is evaluated by aggregating evaluation rollouts with $p = 0$ and $p = 1$, respectively. The other algorithms are evaluated for p sampled from a discretized uniform distribution. If the communication level is not explicitly referred, then the values correspond to the average performance across all communication levels. We refer to Appendix B for a complete description of the experimental methodology, including hyperparameters of the predictive model and the RL controllers. Our code is available on Github.

4.3 RESULTS

We present the main evaluation results in Table 1. For each environment, RL algorithm and method, we present the values of the accumulated rewards obtained. The values that are not significantly different than the highest are presented in bold. The results show that MARO consistently performs equal or better than the MD baseline across all scenarios and algorithms. MARO is able to exploit the information provided by the other agents, in contrast with the fully decentralized approaches (Obs.). Moreover, MARO is often able to achieve performances comparable to the fully centralized agent (J. Obs.), which executes with full communication, despite failures in communication. We also note here that, in some MARL environments, information sharing between agents may not lead to performance gains. For instance, in the SpeakerListener scenario, decentralized QMIX (Obs.) is able to perform competitively in comparison to centralized QMIX (J. Obs.), without requiring information sharing.

In Fig. 2, we highlight the training curves and the performance of the approaches for different communication levels p for the HearSee and SpreadXY environments (more in Appendix B). The results show that MARO outperforms the MD baseline in terms of sample efficiency, with a bigger jump-start in the initial stages of the training (Fig. 2a), and overall performance across all communication levels (Fig. 2b). Additionally, MARO significantly outperforms the Obs. baseline in settings with no communication ($p = 0$); MD struggles to act in the same setting, performing worse than the fully decentralized baseline. Moreover, the performance of MARO improves as the level of communication in the environment increases, showing that our model is able to efficiently make use of all provided information. Appendix B includes all training curves and performance results.

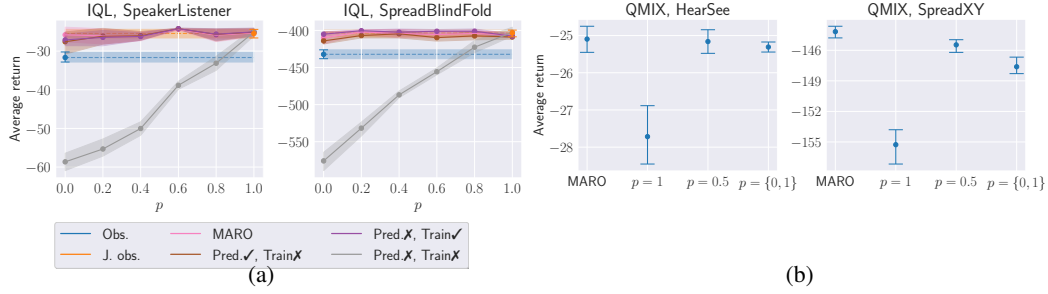


Figure 3: (a) Average episodic returns with 95% confidence interval for different communication levels at execution time for the ablated versions of MARO; (b) Average episodic returns with 95% confidence interval for different sampling schemes. Best viewed with zoom.

Table 2: Average episodic returns and 95% bootstrapped confidence interval over five seeds for all versions of MARO in all scenarios. Higher is better.

Environment	IQL				QMIX			
	MARO	Pred. \checkmark Train \checkmark	Pred. \times Train \checkmark	Pred. \times Train \times	MARO	Pred. \checkmark Train \checkmark	Pred. \times Train \checkmark	Pred. \times Train \times
SpreadXY	-148.7 (-0.7,+0.7)	-158.1 (-0.6,+0.6)	-146.4 (-0.6,+0.7)	-197.4 (-1.7,+1.8)	-144.2 (-0.5,+0.6)	-155.3 (-1.5,+1.9)	-144.4 (-1.1,+1.7)	-197.8 (-1.7,+1.7)
SpreadBlindfold	-405.3 (-4.3,+3.4)	-408.6 (-3.0,+3.0)	-402.9 (-1.8,+2.1)	-479.2 (-2.0,+2.4)	-401.2 (-6.4,+6.4)	-393.8 (-5.2,+4.8)	-407.7 (-5.9,+6.9)	-479.6 (-3.9,+4.3)
HearSee	-25.9 (-0.3,+0.3)	-27.7 (-0.5,+0.5)	-26.1 (-0.3,+0.3)	-78.0 (-4.2,+2.6)	-25.1 (-0.3,+0.4)	-27.7 (-0.8,+0.7)	-25.1 (-0.3,+0.3)	-79.4 (-3.4,+3.4)
SpeakerListener	-25.6 (-0.5,+0.6)	-25.8 (-0.7,+0.7)	-25.8 (-0.7,+0.7)	-43.5 (-0.9,+0.9)	-23.3 (-1.1,+1.3)	-23.5 (-1.2,+1.4)	-23.3 (-1.2,+1.4)	-39.0 (-1.5,+1.7)

4.4 ABLATION STUDY

We perform an ablation study on the two components of MARO to study their impact on the overall performance of the method. We introduce ablated versions of MARO along two different axes: (i) training with our proposed scheme (**Train \checkmark**), against training with fixed $p = 1$ (**Train \times**); and (ii) using the predictive model to estimate missing observations (**Pred \checkmark**), against a naive dropout approach that replaces missing observations with zeros (**Pred \times**). Table 2 shows the results of the ablation study across environments and algorithms. We discuss the results along each axis separately.

4.4.1 TRAINING SCHEME

The results in Table 2 highlight the importance of the training scheme for hybrid execution: introducing our proposed training scheme (**Pred \times , Train \checkmark**) over the fully-ablated version of MARO (**Pred \times , Train \times**) results in a significant performance improvement, while removing the training scheme from MARO (**Pred \checkmark , Train \times**) reduces the performance of our approach.

In Fig. 3a we evaluate the impact of the training scheme in the performance across different communication levels, shown for the SpeakerListener and SpreadBlindfold environments (additional results in Appendix B). The results reveal that MARO is able to perform well across the whole communication spectrum. The results also show that while the fully-ablated version of our approach struggles to act with any communication level other than $p = 1$, adding MARO’s training scheme alone results in a method that is able to perform close to optimally across the entire spectrum of p . Finally, removing the training scheme from MARO results in a performance drop, especially for $p = 0$. In summary, the training scheme is beneficial for different values of p without sacrificing performance for $p = 1$.

We also evaluate the impact of different sampling strategies of p during training. As previously explained, our proposed communication sampling scheme has $p \sim \mathcal{U}(0, 1)$ during training. In Fig. 3b, we compare our sampling scheme in the HearSee and SpreadXY environments (more in Appendix B) against three other sampling approaches: a categorical distribution over the communication level

extremes, $p \sim \mathcal{U}\{0, 1\}$; a fixed sampling scheme with $p = 0.5$, which corresponds to the training approach of Kim et al. (2019b) with additional observation masks; and a fixed sampling scheme with $p = 1$, without observation masks. The results highlight the importance of simulating faulty communication during the training phase, as the fully centralized training scheme ($p = 1$) is outperformed by all other approaches. In Appendix B, we present the full results of this evaluation, showing the impact of the sampling scheme in other scenarios and RL algorithms.

4.4.2 PREDICTIVE MODEL

The results in Table 2 also highlight the significant improvement in the performance of MARO when employing the predictive model to estimate the missing observations. Specifically, adding the predictive model (**Pred ✓, Train ✗**) to the fully ablated version of MARO (**Pred ✗, Train ✗**) results in a significant performance increase. Removing the predictive component from MARO (**Pred ✗, Train ✓**) still results in a competitive algorithm without a significant performance drop in the majority of scenarios. However, there are significant advantages to employing the predictive model:

- The predictive model improves the sample efficiency of MARO. In Fig. 4c, we show the training curves for MARO, with and without the predictive model. The results show that employing the predictive model results in a significant jump-start in terms of sample efficiency. The predictive model provides the RL controllers with an estimate of the missing agent trajectories, instead of replacing the missing input with zeros, resulting in improved performance during the initial stages of the training. This improvement is consistent across several environments and algorithms, as shown in Appendix B.
- The predictive model provides robustness to centralized execution methods when performing tasks in settings with potential faulty communication, despite never being trained to execute in such conditions. In other words, the predictive model allows for zero-shot multi-agent execution with respect to the communication failures. In Fig. 4d, we show that employing the predictive model to predict missing information at execution time allows a standard centralized method to perform the task with minimum performance loss (**Pred ✗, Train ✗**).
- The predictive model is able to perform accurate agent modelling with faulty communication, providing an interpretable insight into the decision-making process of the agents. In Fig. 4a, we show the predicted trajectories of all agents in the perspective of the blue agent, which are close to the real trajectories performed by all agents (more in Appendix B.3.4).

We can also assess the correctness of the predictions made by the predictive model by evaluating the performance of MARO against a *Switch* baseline. In this baseline, the agents choose actions using two controllers, selected accordingly to the level of communication in the environment at each timestep: one that uses the joint observation at the timesteps it is available (similar to the Joint Observation baseline), and one that uses only the local observation, otherwise (similar to the Observation baseline). We show the results of the comparison in performance between MARO and the Switch baseline in Fig. 4b. The results reveal that MARO is able to exploit the predicted observations for communication levels $p < 1$, outperforming the Switch baseline in different communication settings.

5 RELATED WORK

In this section, we connect our work with other lines of research, discussing the similarities and differences between our study and previous works in the field. Due to space limitations, we discuss only the most relevant works and provide an extended discussion of related work in Appendix A.

Closely related to our work are studies that address the problem of partial observability in MARL. As an example, Omidshafiei et al. (2017) propose a decentralized MARL algorithm that uses RNNs to improve the agents’ observability. Mao et al. (2020) use an RNN to compress the agents’ histories, helping to improve agents’ observability. The commonly used paradigm of centralized training with decentralized execution also contributes to alleviating partial observability at training time (Oliehoek et al., 2011; Rashid et al., 2018; Foerster et al., 2016; 2017). Other lines of research investigate communication techniques for MARL (Zhu et al., 2022), focusing on how (Niu et al., 2021; Kim et al., 2019a), when (Singh et al., 2018; Hu et al., 2020), and what (Foerster et al., 2016) to communicate to foster cooperation. Previous studies focused on the sharing of (encoded) local

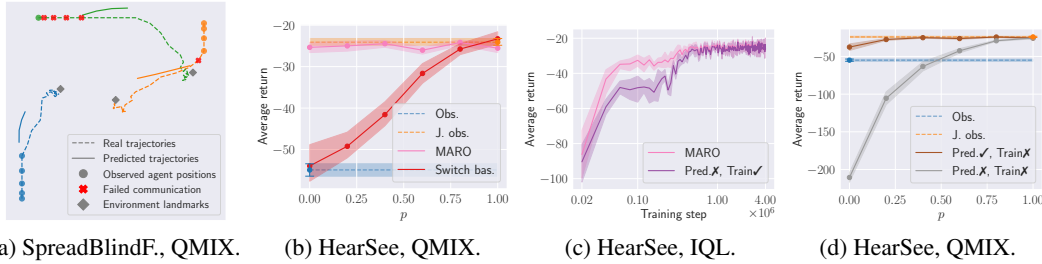


Figure 4: Evaluation of the predictive model of MARO: (a) Trajectory estimation from the perspective of the blue agent, using its agent-specific predictive model; (b) Average episodic returns with 95% confidence interval for different communication levels at execution time of MARO against the Switch baseline; (c) Average episodic returns during training with 95% bootstrapped confidence interval for MARO and an ablated version without the predictive model; (d) Average episodic returns with 95% confidence interval for different communication levels at execution time of ablated versions of MARO, showing the ability of the predictive model for zero-shot execution. Best viewed with zoom.

observations and actions among agents (Foerster et al., 2016) in a proxy-like manner (Wang et al., 2019). Previous works consider learning robust communication protocols under missing information. Studies learn mechanisms that improve communication efficiency by either limiting the variance of exchanged messages (Zhang et al., 2019) or temporally smoothing information shared between agents (Zhang et al., 2020). Kim et al. (2019b) propose message-dropout, which aims at making learning robust against communication errors. Message-dropout drops the messages received from other agents independently at random during training before inputting them into the RL algorithm. In a similar fashion to message dropout, Wang et al. (2020) propose a recurrent actor-critic algorithm for handling multi-agent coordination under partial observability with limited communication, showing that recurrency successfully contributes to robust performance under communication failures.

In contrast, we assume that agents have no control over when and with whom to communicate. Hence, they should robustly perform under any type of communication policy/level at execution time. Also, we do not learn the content of the messages and consider a rather passive communication setting in which agents share local observations and actions. For this reason, we did not include the works of Zhang et al. (2019) and Zhang et al. (2020) as baselines since the comparison between methods would not be meaningful. Instead, following both Kim et al. (2019b) and Wang et al. (2020), we use message-dropout with recurrent learners as a baseline. Finally, none of the aforementioned works proposed the use of predictive models to account for missing information at execution time as we do in our work, nor mathematically formalized hybrid execution as we present in Sec. 2.1.

Other lines of research are also relevant to our work. As opposed to agent/opponent modelling Papoudakis et al. (2021a); Xie et al. (2020); He et al. (2016), we aim at learning policies for multiple agents concurrently. In contrast to multi-agent trajectory prediction (Alahi et al., 2016; Yeh et al., 2019; Hauri et al., 2020; Omidshafiei et al., 2021), we consider a rather broader setting in which agents’ observations can correspond to any type of information collected by the agents and use the predictive model with the objective of being robust to missing information. Finally, while our method can be categorized as a model-based MARL method (Bargiacchi et al., 2021; Kim et al., 2021; Wang et al., 2022), as opposed to previous works which are mainly focused on using the model to increase sample efficiency, we use the predictive model with the objective of estimating missing observations.

6 CONCLUSION

In this work, we introduce *hybrid* execution, a new paradigm in which agents act under any communication level at execution time, while exploiting information-sharing among the agents. To formalize our setting, we define hybrid-POMDPs, a new class of POMDPs that explicitly considers a communication process between the agents. To allow for hybrid execution we propose MARO, a novel approach that combines an autoregressive predictive model, to estimate missing observations, and an RL training scheme that randomly drops agent observations, simulating different communication

levels during the centralized training phase. We show that MARO allows agents to act across different communication levels, successfully exploiting available shared information.

Future work could comprise: (i) evaluating MARO with actor-critic RL algorithms; (ii) studying other neural network architectures, such as graph neural networks, for better multi-agent trajectory prediction; (iii) studying the performance of MARO under other communication settings.

ACKNOWLEDGEMENTS

This work was partially supported by Portuguese national funds through the Portuguese Fundação para a Ciência e a Tecnologia (FCT) under projects UIDB/50021/2020 (INESC-ID multi-annual funding), PTDC/CCI-COM/5060/2021 (RELEvaNT), PTDC/CCI-COM/7203/2020 (HOTSPOT), and PTDC/CCI-COM/30787/2017 (SLICE). In addition, this research was partially supported by TAILOR, a project funded by EU Horizon 2020 research and innovation programme under GA No. 952215, and by the Air Force Office of Scientific Research under award number FA9550-22-1-0475. Pedro P. Santos acknowledges the FCT PhD grant 2021.04684.BD. Diogo S. Carvalho acknowledges the FCT PhD grant 2020.05360.BD. Miguel Vasco acknowledges the FCT PhD grant SFRH/BD/139362/2018.

REFERENCES

- Alexandre Alahi, Kratarth Goel, Vignesh Ramanathan, Alexandre Robicquet, Li Fei-Fei, and Silvio Savarese. Social lstm: Human trajectory prediction in crowded spaces. In *2016 IEEE Conference on Computer Vision and Pattern Recognition (CVPR)*, 2016.
- Eugenio Bargiacchi, Timothy Verstraeten, and Diederik M. Roijers. Cooperative prioritized sweeping. In *Proceedings of the 20th International Conference on Autonomous Agents and MultiAgent Systems*, pp. 160–168, 2021.
- Lorenzo Canese, Gian Carlo Cardarilli, Luca Di Nunzio, Rocco Fazzolari, Daniele Giardino, Marco Re, and Sergio Spanò. Multi-agent reinforcement learning: A review of challenges and applications. *Applied Sciences*, 11(11), 2021.
- Xiaohan Fang, Jinkuan Wang, Guanru Song, Yinghua Han, Qiang Zhao, and Zhiao Cao. Multi-agent reinforcement learning approach for residential microgrid energy scheduling. *Energies*, 13(1), 2020.
- Jakob N. Foerster, Yannis M. Assael, Nando de Freitas, and Shimon Whiteson. Learning to communicate with deep multi-agent reinforcement learning. *CoRR*, abs/1605.06676, 2016.
- Jakob N. Foerster, Gregory Farquhar, Triantafyllos Afouras, Nantas Nardelli, and Shimon Whiteson. Counterfactual multi-agent policy gradients. *CoRR*, abs/1705.08926, 2017.
- Sandro Hauri, Nemanja Djuric, Vladan Radosavljevic, and Slobodan Vucetic. Multi-modal trajectory prediction of NBA players. *CoRR*, abs/2008.07870, 2020.
- He He, Jordan Boyd-Graber, Kevin Kwok, and Hal Daumé III. Opponent modeling in deep reinforcement learning. In *International conference on machine learning*, pp. 1804–1813. PMLR, 2016.
- Florence Ho, Ana Salta, Ruben Geraldes, Artur Goncalves, Marc Cavazza, and Helmut Prendinger. Multi-agent path finding for uav traffic management. In *Proceedings of the 18th International Conference on Autonomous Agents and MultiAgent Systems*, pp. 131–139, 2019.
- Guangzheng Hu, Yuanheng Zhu, Dongbin Zhao, Mengchen Zhao, and Jianye Hao. Event-triggered multi-agent reinforcement learning with communication under limited-bandwidth constraint. *CoRR*, abs/2010.04978, 2020.
- Jiechuan Jiang and Zongqing Lu. Learning attentional communication for multi-agent cooperation. *CoRR*, abs/1805.07733, 2018.

-
- Daewoo Kim, Sangwoo Moon, David Hostallero, Wan Ju Kang, Taeyoung Lee, Kyunghwan Son, and Yung Yi. Learning to schedule communication in multi-agent reinforcement learning. *CoRR*, abs/1902.01554, 2019a.
- Woojun Kim, Myungsik Cho, and Youngchul Sung. Message-dropout: An efficient training method for multi-agent deep reinforcement learning. *CoRR*, abs/1902.06527, 2019b.
- Woojun Kim, Jongeui Park, and Youngchul Sung. Communication in multi-agent reinforcement learning: Intention sharing. In *International Conference on Learning Representations*, 2021.
- Ryan Lowe, Yi I Wu, Aviv Tamar, Jean Harb, OpenAI Pieter Abbeel, and Igor Mordatch. Multi-agent actor-critic for mixed cooperative-competitive environments. *Advances in neural information processing systems*, 30, 2017.
- Weichao Mao, Kaiqing Zhang, Erik Miehling, and Tamer Basar. Information state embedding in partially observable cooperative multi-agent reinforcement learning. *CoRR*, abs/2004.01098, 2020.
- Yaru Niu, Rohan Paleja, and Matthew Gombolay. Multi-agent graph-attention communication and teaming. In *Proceedings of the 20th International Conference on Autonomous Agents and MultiAgent Systems*, pp. 964–973, 2021.
- Frans A. Oliehoek and Christopher Amato. *A concise introduction to decentralized POMDPs*. Springer, 2016.
- Frans A. Oliehoek, Matthijs T. J. Spaan, and Nikos Vlassis. Optimal and approximate q-value functions for decentralized pomdps. *CoRR*, abs/1111.0062, 2011.
- Shayegan Omidshafiei, Jason Pazis, Christopher Amato, Jonathan P. How, and John Vian. Deep decentralized multi-task multi-agent reinforcement learning under partial observability. In *Proceedings of the 34th International Conference on Machine Learning*, pp. 2681–2690, 2017.
- Shayegan Omidshafiei, Daniel Hennes, Marta Garnelo, Eugene Tarassov, Zhe Wang, Romuald Elie, Jerome T. Connor, Paul Muller, Ian Graham, William Spearman, and Karl Tuyls. Time-series imputation of temporally-occluded multiagent trajectories. *CoRR*, abs/2106.04219, 2021.
- Georgios Papoudakis, Filippas Christianos, Lukas Schäfer, and Stefano V. Albrecht. Comparative evaluation of multi-agent deep reinforcement learning algorithms. *CoRR*, abs/2006.07869, 2020.
- Georgios Papoudakis, Filippas Christianos, and Stefano Albrecht. Agent modelling under partial observability for deep reinforcement learning. *Advances in Neural Information Processing Systems*, 34:19210–19222, 2021a.
- Georgios Papoudakis, Filippas Christianos, Lukas Schäfer, and Stefano V Albrecht. Benchmarking multi-agent deep reinforcement learning algorithms in cooperative tasks. In *Thirty-fifth Conference on Neural Information Processing Systems Datasets and Benchmarks Track (Round 1)*, 2021b.
- Adam Paszke, Sam Gross, Francisco Massa, Adam Lerer, James Bradbury, Gregory Chanan, Trevor Killeen, Zeming Lin, Natalia Gimelshein, Luca Antiga, Alban Desmaison, Andreas Kopf, Edward Yang, Zachary DeVito, Martin Raison, Alykhan Tejani, Sasank Chilamkurthy, Benoit Steiner, Lu Fang, Junjie Bai, and Soumith Chintala. Pytorch: An imperative style, high-performance deep learning library. In *Advances in Neural Information Processing Systems 32*, pp. 8024–8035. 2019.
- Tabish Rashid, Mikayel Samvelyan, Christian Schröder de Witt, Gregory Farquhar, Jakob N. Foerster, and Shimon Whiteson. QMIX: monotonic value function factorisation for deep multi-agent reinforcement learning. *CoRR*, abs/1803.11485, 2018.
- Amanpreet Singh, Tushar Jain, and Sainbayar Sukhbaatar. Learning when to communicate at scale in multiagent cooperative and competitive tasks. *CoRR*, abs/1812.09755, 2018.
- Sainbayar Sukhbaatar, Arthur Szlam, and Rob Fergus. Learning multiagent communication with backpropagation. *CoRR*, abs/1605.07736, 2016.
- Ming Tan. Multi-agent reinforcement learning: Independent vs. cooperative agents. In *Proceedings of the tenth international conference on machine learning*, pp. 330–337, 1993.

-
- Rose E. Wang, Michael Everett, and Jonathan P. How. R-MADDPG for partially observable environments and limited communication. *CoRR*, abs/2002.06684, 2020.
- Rundong Wang, Xu He, Runsheng Yu, Wei Qiu, Bo An, and Zinovi Rabinovich. Learning efficient multi-agent communication: An information bottleneck approach. *CoRR*, abs/1911.06992, 2019.
- Xihuai Wang, Zhicheng Zhang, and Weinan Zhang. Model-based multi-agent reinforcement learning: Recent progress and prospects, 2022.
- Hua Wei, Guanjie Zheng, Vikash V. Gayah, and Zhenhui Li. A survey on traffic signal control methods. *CoRR*, abs/1904.08117, 2019.
- Daniël Willemsen, Mario Coppola, and Guido C.H.E. de Croon. Mambpo: Sample-efficient multi-robot reinforcement learning using learned world models. In *2021 IEEE/RSJ International Conference on Intelligent Robots and Systems (IROS)*, pp. 5635–5640, 2021.
- Annie Xie, Dylan P Losey, Ryan Tolsma, Chelsea Finn, and Dorsa Sadigh. Learning latent representations to influence multi-agent interaction. *arXiv preprint arXiv:2011.06619*, 2020.
- Raymond A. Yeh, Alexander G. Schwing, Jonathan Huang, and Kevin Murphy. Diverse generation for multi-agent sports games. In *2019 IEEE/CVF Conference on Computer Vision and Pattern Recognition (CVPR)*, pp. 4605–4614, 2019. doi: 10.1109/CVPR.2019.00474.
- Ekim Yurtsever, Jacob Lambert, Alexander Carballo, and Kazuya Takeda. A survey of autonomous driving: Common practices and emerging technologies. *IEEE access*, 8:58443–58469, 2020.
- Sai Qian Zhang, Qi Zhang, and Jieyu Lin. Efficient communication in multi-agent reinforcement learning via variance based control. *CoRR*, abs/1909.02682, 2019.
- Sai Qian Zhang, Jieyu Lin, and Qi Zhang. Succinct and robust multi-agent communication with temporal message control. *CoRR*, abs/2010.14391, 2020.
- Changxi Zhu, Mehdi Dastani, and Shihan Wang. A survey of multi-agent reinforcement learning with communication, 2022.

A EXTENDED RELATED WORK

In this section, we connect our work with other lines of research, discussing the similarities and differences between our study and previous works in the field. The discussion herein presented corresponds to an extended version of Sec. 5.

A.1 PARTIAL OBSERVABILITY IN MARL

Closely related to our work are studies that address the problem of partial observability in MARL. As an example, Omidshafiei et al. (2017) propose a decentralized MARL algorithm that uses RNNs to improve the agents’ observability. Mao et al. (2020) use an RNN to first compress the agents’ histories into embeddings that are posteriorly fed into deep Q-networks, helping to improve agents’ observability. The commonly used paradigm of centralized training with decentralized execution also contributes to alleviating partial observability at train time (Oliehoek et al., 2011; Rashid et al., 2018; Foerster et al., 2016; 2017). Under such paradigm, the calculation of value functions or policy gradients can exploit the centralization of information, thus alleviating partial observability.

Another way to alleviate the problem of partial observability in MARL, especially at test time, is to consider communication between the agents. We review such setting in the following section.

A.1.1 COMMUNICATION IN MARL

Different lines of research focus their attention on the development of communication techniques for MARL (Zhu et al., 2022), focusing on how the sharing of information between the agents can be used to improve the RL agents’ learning. Early works addressed communication under partially observable cooperative MARL tasks: Sukhbaatar et al. (2016) share the outputs of the hidden layers of a shared neural network among the agents; Foerster et al. (2016) explicitly learn the content of the messages transmitted between agents by following an end-to-end approach in which gradients are back-propagated through the communication variables. Recent works in the field study how (Niu et al., 2021; Kim et al., 2019a), when (Singh et al., 2018; Hu et al., 2020), and what (Foerster et al., 2016) should be communicated among the agents in order to foster cooperation.

Similarly to our work, previous studies focused on the sharing of (encoded) local observations and actions among agents (Foerster et al., 2016) in a proxy-like manner (Wang et al., 2019). However, as opposed to previous works, we assume that agents have no control over when and with whom to communicate and, instead, should robustly perform under any type of communication policy. We also emphasize that we are not focused on learning the content of the messages being communicated (as in (Foerster et al., 2016)), focusing our attention on a rather “passive” communication setting by considering the sharing of local observations and actions among the agents. Other works focus on learning how to combine received information with local information before feeding it into the RL model (Jiang & Lu, 2018; Wang et al., 2019). In our work, we concatenate received information alongside local information. However, the methods developed by previous studies, which can be seen as orthogonal contributions in comparison to our work, can be readily incorporated into our method.

Finally, some works consider learning robust communication protocols under failing/missing information. Previous studies learn mechanisms that improve communication efficiency by either limiting the variance of exchanged messages (Zhang et al., 2019), or temporally smoothing information shared between agents (Zhang et al., 2020). Due to the decreased variability of the messages exchanged throughout timesteps, such methods achieve improved robustness against transmission loss. However, since in this work we are not focusing our attention on methods that learn the contents of the messages being exchanged, we did not use the aforementioned methods as baselines in our work as the comparison between methods would be deemed inappropriate. Kim et al. (2019b) propose a learning technique for MARL called message-dropout, which aims at: (i) effectively handling the increased input dimension in MARL with communication; and (ii) making learning robust against communication errors in the execution phase. Message-dropout drops the messages received from other agents independently at random during training before inputting them into the RL algorithm. In a similar fashion to message dropout, Wang et al. (2020) propose a recurrent actor-critic algorithm for handling multi-agent coordination under partial observability with limited communication, showing that recurrency successfully contributes to robust performance when communication fails. Following

both Kim et al. (2019b) and Wang et al. (2020), we use message-dropout with recurrent learners as a baseline in our work.

We refer to Zhu et al. (2022) for an extensive discussion of the different works that propose communication protocols for MARL.

A.2 MODELLING OTHER AGENTS

In contexts where a single agent learns in an environment where other agents are also present, some works have explored ways to model information about the other agents, such as their actions and observations, based on local information available to the learning agent. The work of Papoudakis et al. (2021a) uses a recurrent neural network to predict the other agents’ actions and observations in order to make better action selections in a centralized training with decentralized execution setting. At execution time, the agent then uses its learned model to make explicit predictions about other agents’ observations and actions. Xie et al. (2020) does similarly in a latent space. The work of He et al. (2016) uses, instead, the other agents’ observations to predict their actions, which assumes centralization will be available at execution time.

Contrarily to the mentioned settings, in ours, we aim at learning policies for multiple agents. To that end, we use a model of the agents’ observations and actions to make predictions about other agents and improve their performance in cooperative tasks.

A.3 MODEL-BASED MARL

Recently, different works addressed model-based MARL, being mostly focused on improving the sample efficiency of MARL methods by leveraging the knowledge of the learned environment dynamics in policy optimization (Willemssen et al., 2021; Bargiacchi et al., 2021). Closely related to our work are studies that propose model-based approaches to MARL while considering communication among the agents. As an example, Kim et al. (2021) propose a communication protocol that encodes into the message an agent’s imagined trajectory computed by performing rollouts using an opponent model and a dynamics function.

As opposed to previous works, in our work we focus our attention on the study of methods that allow for robust execution under different communication degrees. While our method can be categorized as a model-based MARL method that implicitly models both the dynamics function as well as the other agents’ policies, we use it with a rather different objective than the aforementioned articles.

We refer to Wang et al. (2022) for an extensive discussion of model-based approaches to MARL.

A.4 MULTI-AGENT TRAJECTORY PREDICTION

There exists a number of works that address trajectory prediction under multi-agent settings using sequence models (Alahi et al., 2016; Yeh et al., 2019; Hauri et al., 2020; Omidshafiei et al., 2021). As an example, Alahi et al. (2016) use an RNN to learn and predict the trajectory of pedestrians. Hauri et al. (2020) propose an uncertainty-aware multi-modal deep learning model to predict multiple future trajectories of basketball players. Omidshafiei et al. (2021) propose a method based on graph neural networks and bi-directional RNNs to predict unobserved parts of football players’ trajectories.

Our work resembles some similarities with the aforementioned studies since our predictive method MARO solves a similar problem to that of the aforementioned works if we consider that the observations correspond to agents’ coordinates. However, in our study, we consider a rather broader setting in which agents’ observations can correspond to any type of information collected by the agents. Importantly, we focus our attention on control settings whereas the previous works only deal with predictive settings. Also, we use the predictive model with the objective of being robust to missing information during agency. Nevertheless, we note that our method MARO can possibly benefit from techniques proposed by the aforementioned works.

B EXPERIMENTAL EVALUATION

In this section, we present supplementary materials for Sec. 4. We describe the proposed MARL scenarios in detail in Sec. B.1. In Sec. B.2, we describe our experimental methodology. Finally, we present our complete set of experimental results in Sec. B.3.

B.1 DESCRIPTION OF THE PROPOSED MARL SCENARIOS

Spreadblindfold (SB) The environment consists of three agents and three designated landmarks in a 2D map. At the start of each episode both the position of the agents and of the landmarks is randomly generated. The goal of the agents is to cover all the landmarks while avoiding collisions: agents are (globally) rewarded considering how far the closest agent is to each landmark (sum of the minimum distances) and are (locally) penalized if they collide with other agents. Differently from the original Simple Spread environment, the agent’s observation only includes the position and velocity of the agent itself and the relative position of all landmarks. Through communication with the central proxy, the agents can access the position and velocities of the other agents.

HearSee (HS) The environment consists of two heterogeneous agents and a single landmark in a 2D map. At the start of each episode both the position of the agents and of the landmark is randomly generated. The goal of the agents is to cooperate in order for both of them to cover the landmark: agents are (globally) rewarded considering how far the closest agent is to each landmark (sum of the minimum distances). In this scenario, one of the agents (“Hear” agent) is provided with the absolute position of the landmark in its observation. However, it does not have access to its own position. The other agent (“See” agent) is able to access the position and velocities of both agents in its observation, yet does not have access to the position of the landmark. Only through communicating with the central proxy, can the agents have access to both their positions and the position of the landmark in order to complete the task.

SpreadXY (SXY) The environment consists of two heterogeneous agents and two designated landmarks in a 2D map. At the start of each episode both the position of the agents and of the landmarks is randomly generated. The goal of the agents is to cover all the landmarks while avoiding collisions: agents are (globally) rewarded considering how far the closest agent is to each landmark (sum of the minimum distances) and are (locally) penalized if they collide with other agents. Differently from SSB, one of the agents has access to the X position and velocity of both agents, while the other agent has access to the Y position and velocity of both agents. Both agents observe as well the absolute position of all landmarks. Through communication with the central proxy, the agents can access the complete position and velocities of the other agents and cover the landmarks.

B.2 EXPERIMENTAL METHODOLOGY, IMPLEMENTATION AND HYPERPARAMETERS

We consider two MARL algorithms: IQL and QMIX. We employ the same LSTM-based controller networks across all evaluations. We follow the hyperparameters suggested by Papoudakis et al. (2021b); we train all models for 4M steps, performing 5 training runs for each experimental setting and 50 evaluation rollouts for each training run. We assume that $p = 1$ at $t = 0$ for the MD and MARO algorithms. The performance of the Obs. and J. Obs. baselines are evaluated by aggregating evaluation rollouts with $p = 0$ and $p = 1$, respectively. The other algorithms are evaluated for p sampled from a discretized uniform distribution. We display our training hyperparameters for the RL controllers and the predictive model in Table 3 and Table 4, respectively.

We developed our code in a Python environment using the EPyMARL framework (Papoudakis et al., 2021b) and PyTorch (Paszke et al., 2019). The computational code is available in Github.

B.3 EXPERIMENTAL RESULTS

In this section, we display the complete experimental results. Our main results are presented in Sec. B.3.1; the results of our ablation study are presented in Sec. B.3.2. In Sec. B.3.3, we display the results for the *Switch* baseline. In Sec. B.3.4 we display a set of figures that illustrates the predictions made by the predictive model. In all plots, alongside scalar mean values, we report the 95% bootstrapped confidence interval.

Table 3: Hyperparameters for the RL controllers across all environments.

(a) IQL		(b) QMIX	
hidden dimension	128	hidden dimension	128
learning rate	0.0005	learning rate	0.0005
reward standardisation	True	reward standardisation	True
network type	GRU	network type	GRU
evaluation epsilon	0.0	evaluation epsilon	0.0
epsilon anneal	500,000	epsilon anneal	50,000
target update	200	target update	200

Table 4: Hyperparameters for the predictive model across all environments and algorithms.

hidden dimension	128
learning rate	0.001
grad clip	1.0

B.3.1 MAIN EXPERIMENTAL RESULTS

In this section, we present the complete experimental results of all approaches across all environments and algorithms: in Figs. 5 and 6 we show the performance in all environments of all approaches during training, considering different communication levels p , using the IQL and QMIX algorithms, respectively; in Figs. 7 and 8 we show the performance in all environments of all approaches during training, considering $p \sim \mathcal{U}(0, 1)$, using the IQL and QMIX algorithms, respectively; in Figs. 9 and 10 we show the performance in all environments of all approaches during execution, considering different communication levels p , using the IQL and QMIX algorithms, respectively.

B.3.2 ABLATION STUDY

In this section, we present the complete experimental results of the ablation study of MARO across all environments and algorithms: in Figs. 11 and 12 we show the performance in all environments of MARO and the ablated versions during training, considering different communication levels p , using the IQL and QMIX algorithms, respectively; in Figs. 13 and 14 we show the performance in all environments of MARO and the ablated versions during training, considering $p \sim \mathcal{U}(0, 1)$, using the IQL and QMIX algorithms, respectively; in Figs. 15 and 15 we show the performance in all environments of MARO and the ablated versions during execution, considering different communication levels p , using the IQL and QMIX algorithms, respectively; in Figs. 17 and 18 we show the performance in all environments of different sampling methods for the training scheme of MARO, using the IQL and QMIX algorithms, respectively.

B.3.3 SWITCH BASELINE

In Fig. 19 we present the experimental results that compare MARO against the *Switch* baseline, introduced in Section 4.4.2, in the HearSee environment. The Switch baseline selects actions using two controllers: one that receives the joint observation, used when communication is allowed, and another that receives only the local observation, used otherwise.

B.3.4 MULTI-AGENT TRAJECTORY PREDICTION

We display, in Figs. 20, 21 and 22, an illustration of the trajectory predictions made by the predictive model from the perspective of each of the agents. The plots are computed, at each timestep and from the perspective of each agent, by computing the estimated trajectories of all agents for the next 4 timesteps. The 4-step ahead predictions are entirely computed using estimated quantities, i.e., real observations are not incorporated into the predictions and the predictive model works in a fully auto-regressive manner.

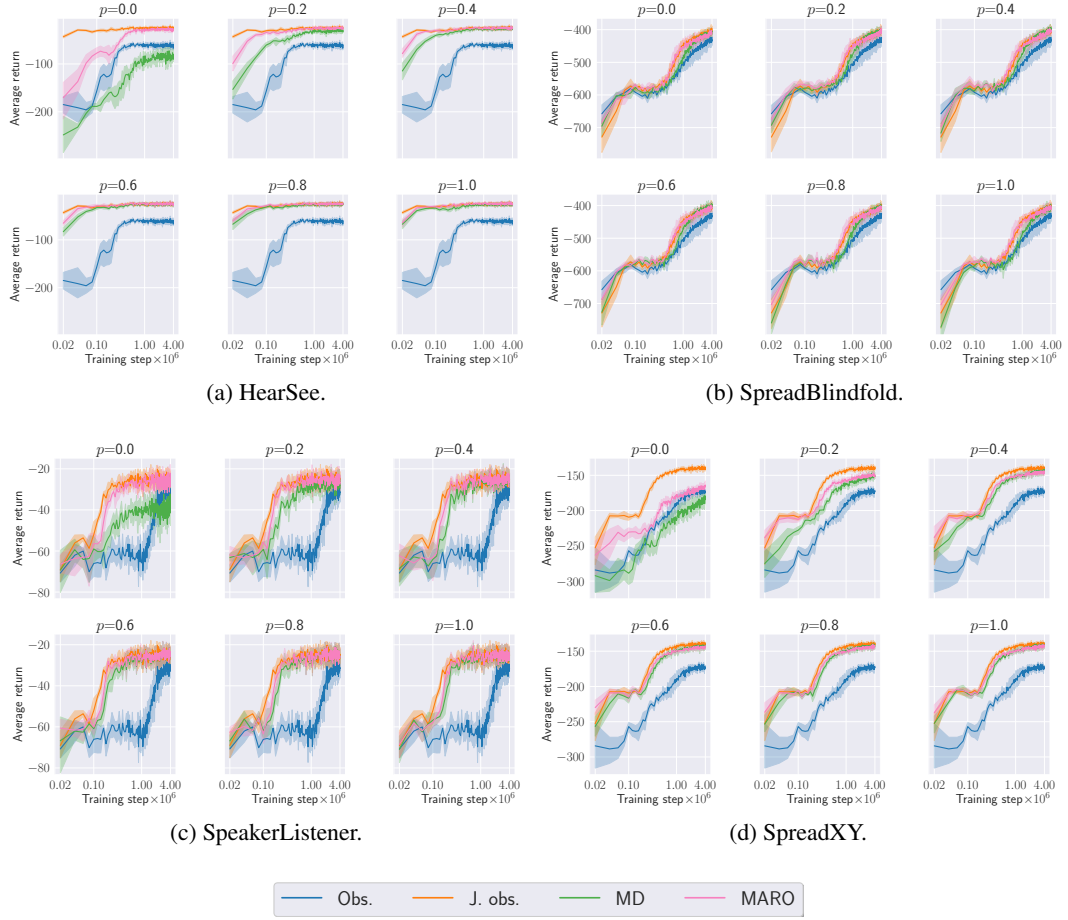


Figure 5: Average episodic returns during training with 95% bootstrapped confidence interval for different communication levels p , for all approaches and environments, using the IQL algorithm.

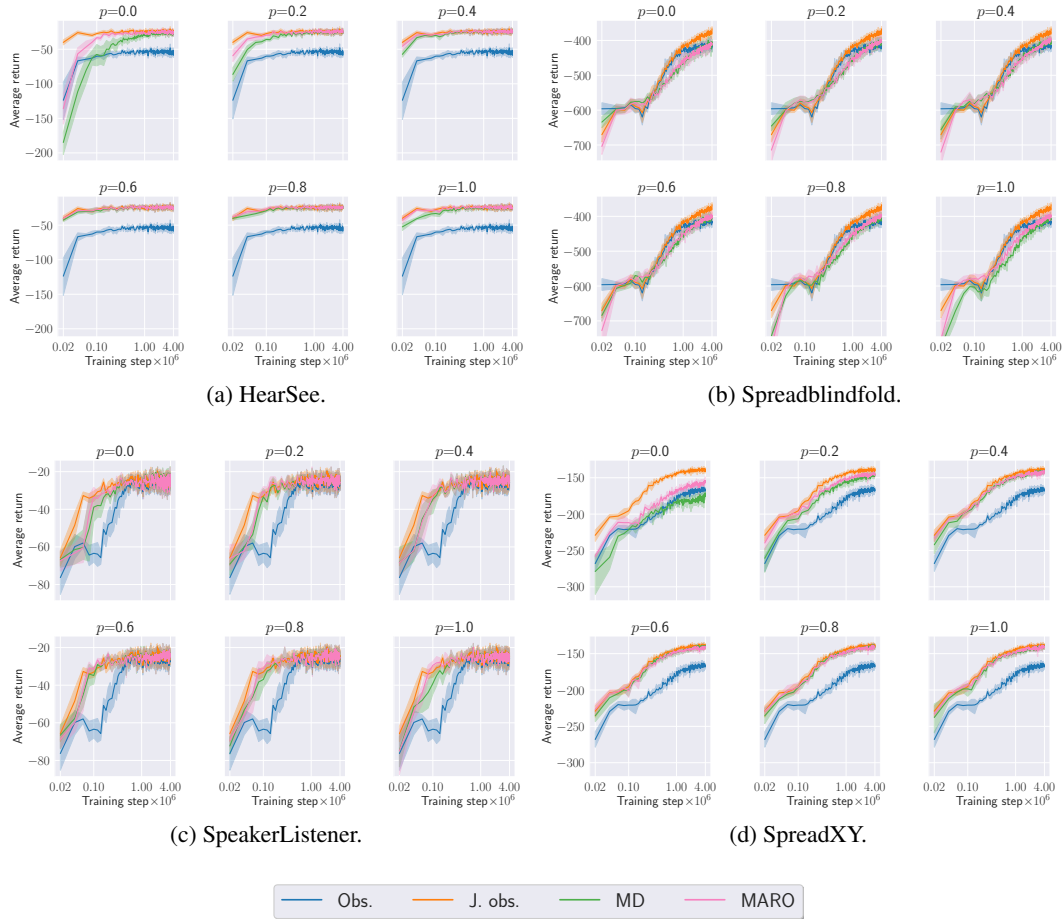


Figure 6: Average episodic returns during training with 95% bootstrapped confidence interval for different communication levels p , for all approaches and environments, using the QMIX algorithm.

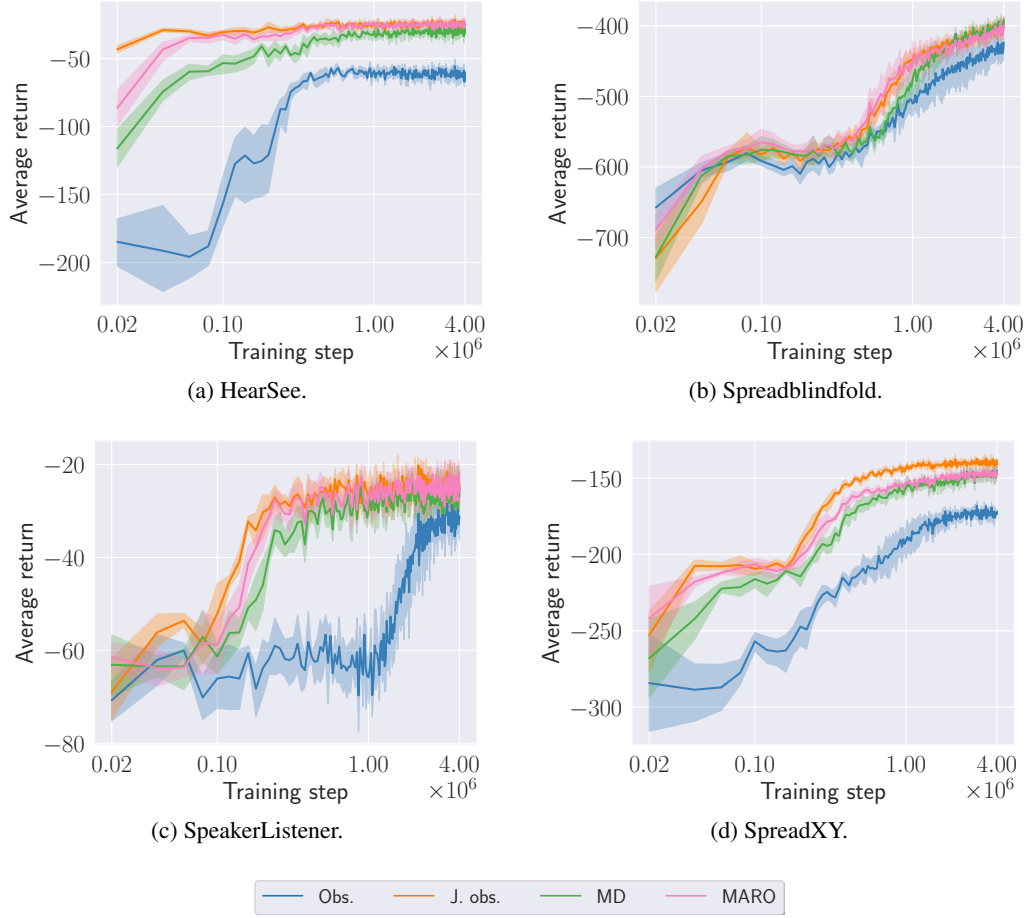


Figure 7: Average episodic returns during training with 95% bootstrapped confidence interval for $p \sim \mathcal{U}(0, 1)$, for all approaches and environments, using the IQL algorithm.

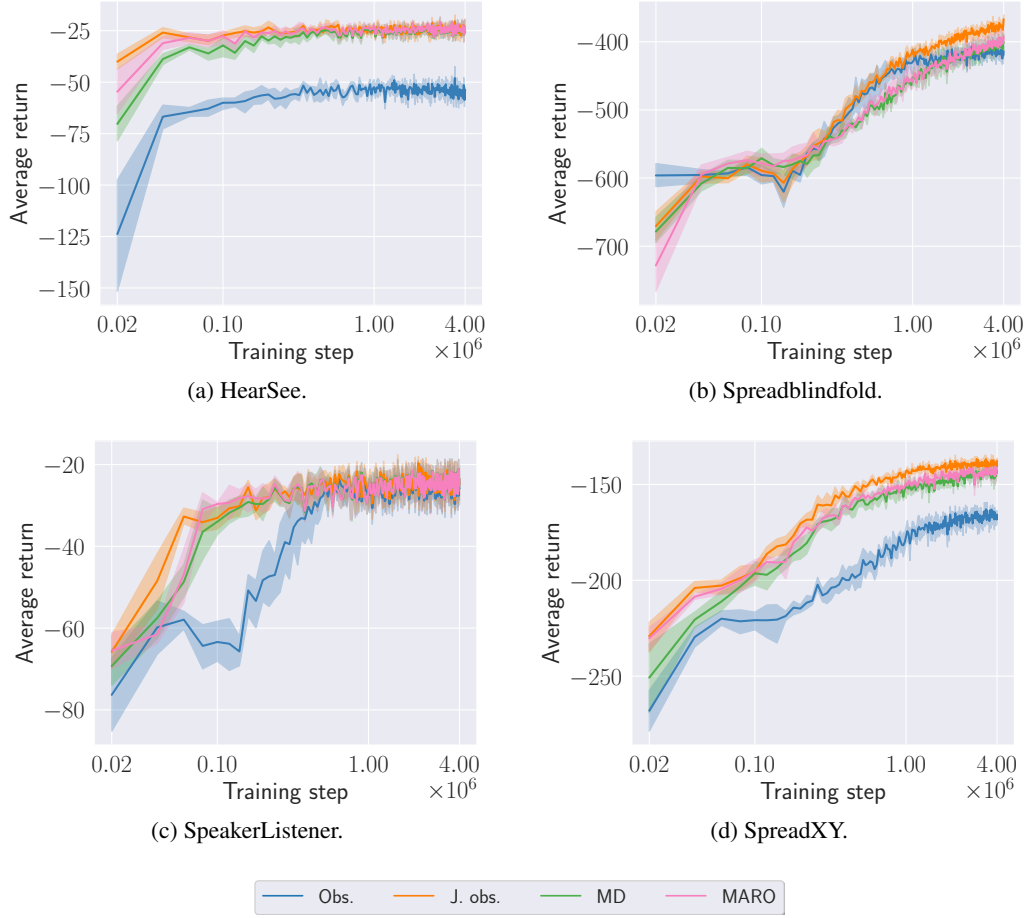


Figure 8: Average episodic returns during training with 95% bootstrapped confidence interval for $p \sim \mathcal{U}(0, 1)$, for all approaches and environments, using the QMIX algorithm.

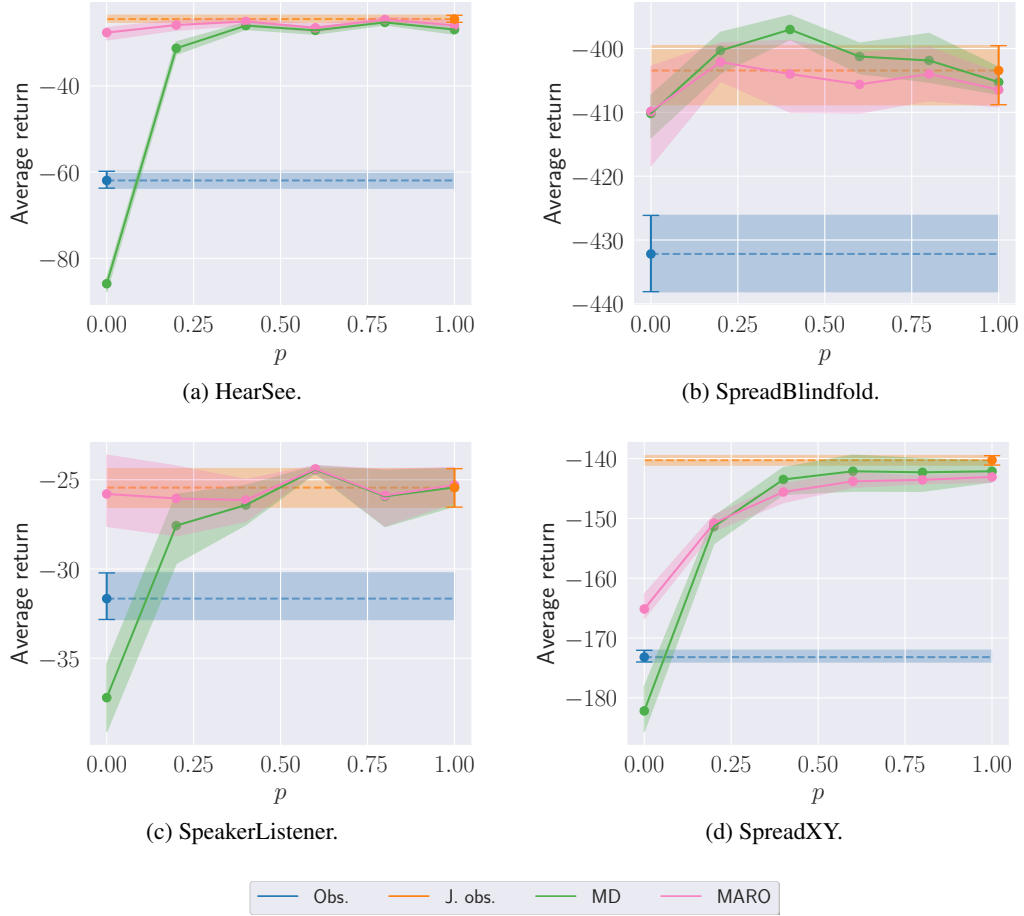


Figure 9: Average episodic returns with 95% bootstrapped confidence interval for different communication levels p at execution time, for all approaches across different environments, using the IQL algorithm.

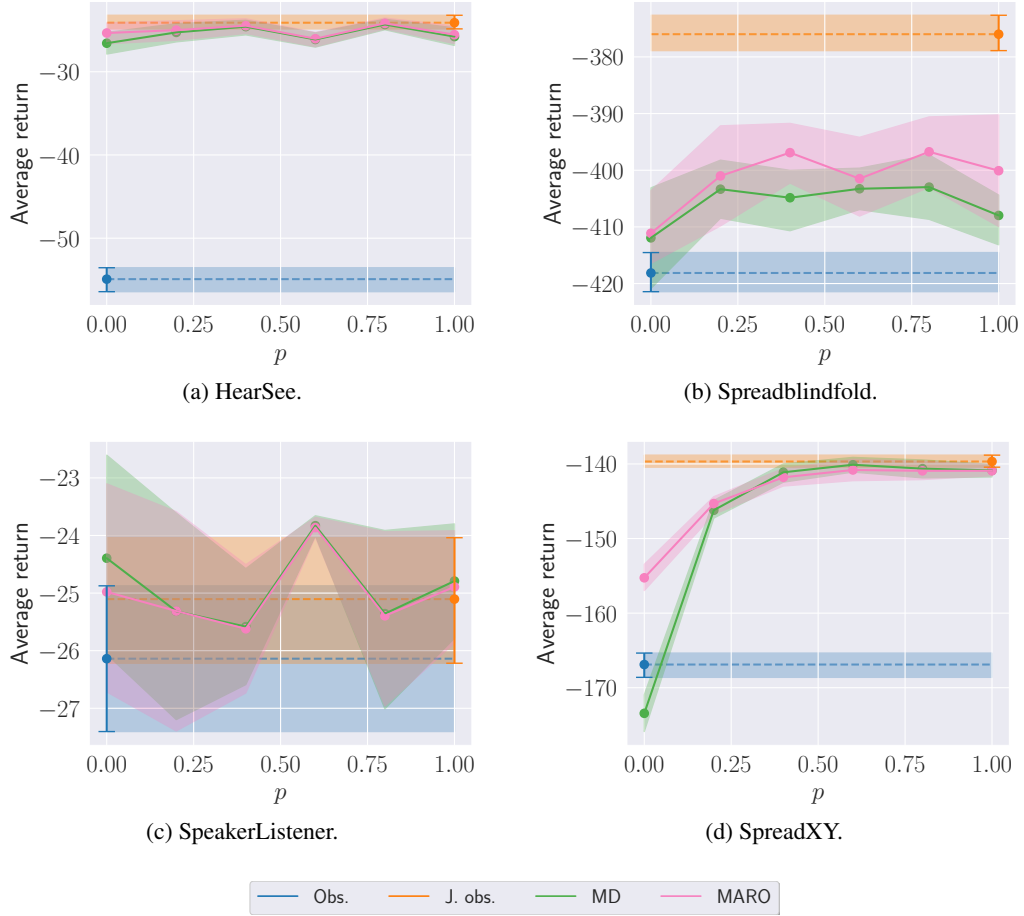


Figure 10: Average episodic returns with 95% bootstrapped confidence interval for different communication levels p at execution time, for all approaches across different environments, using the QMIX algorithm.

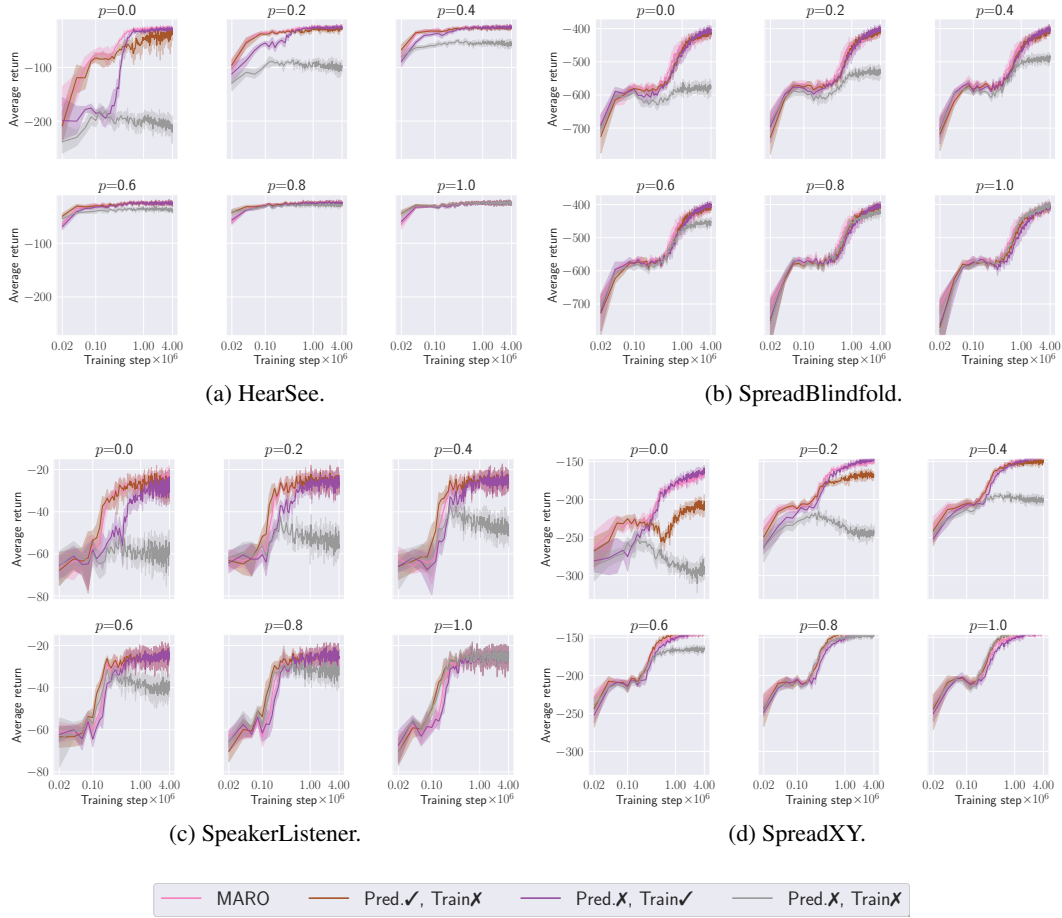


Figure 11: Average episodic returns during training with 95% bootstrapped confidence interval for different communication levels p , for MARO and the ablated versions across all environments, using the IQL algorithm.

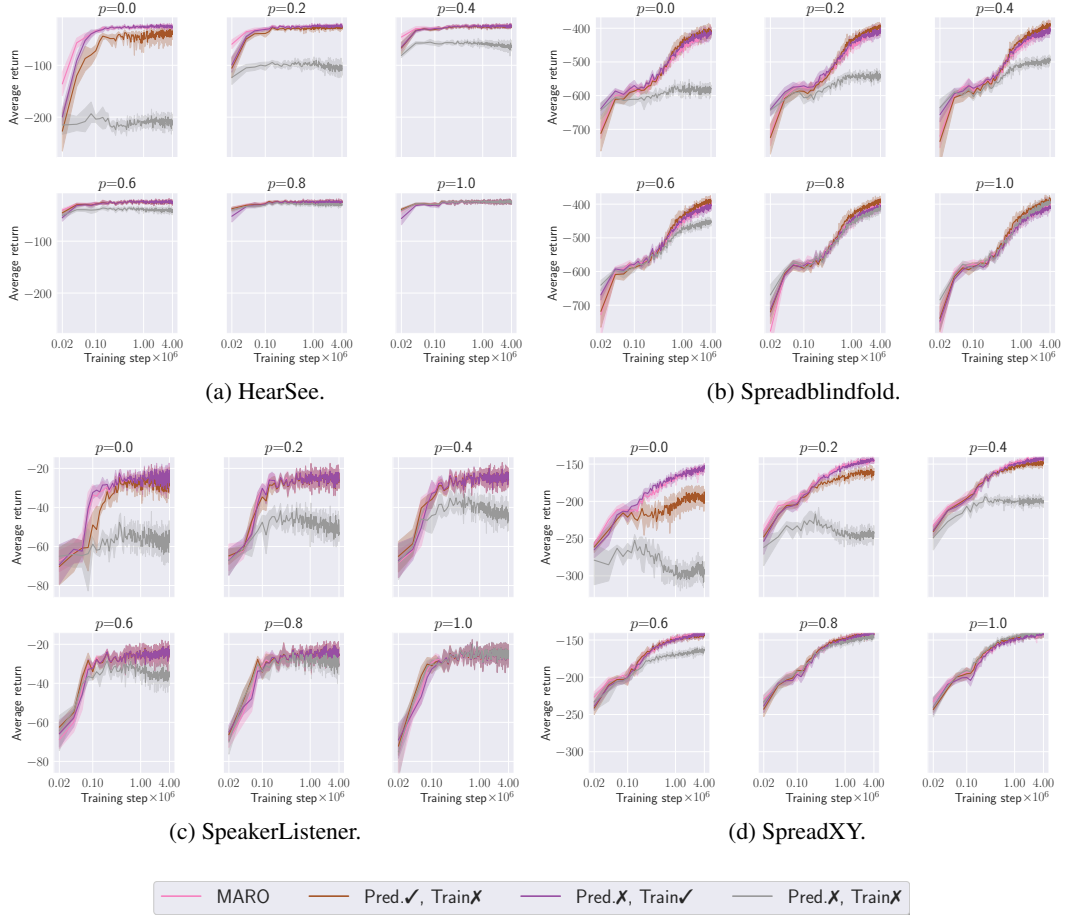


Figure 12: Average episodic returns during training with 95% bootstrapped confidence interval for different communication levels p , for MARO and the ablated versions across all environments, using the QMIX algorithm.

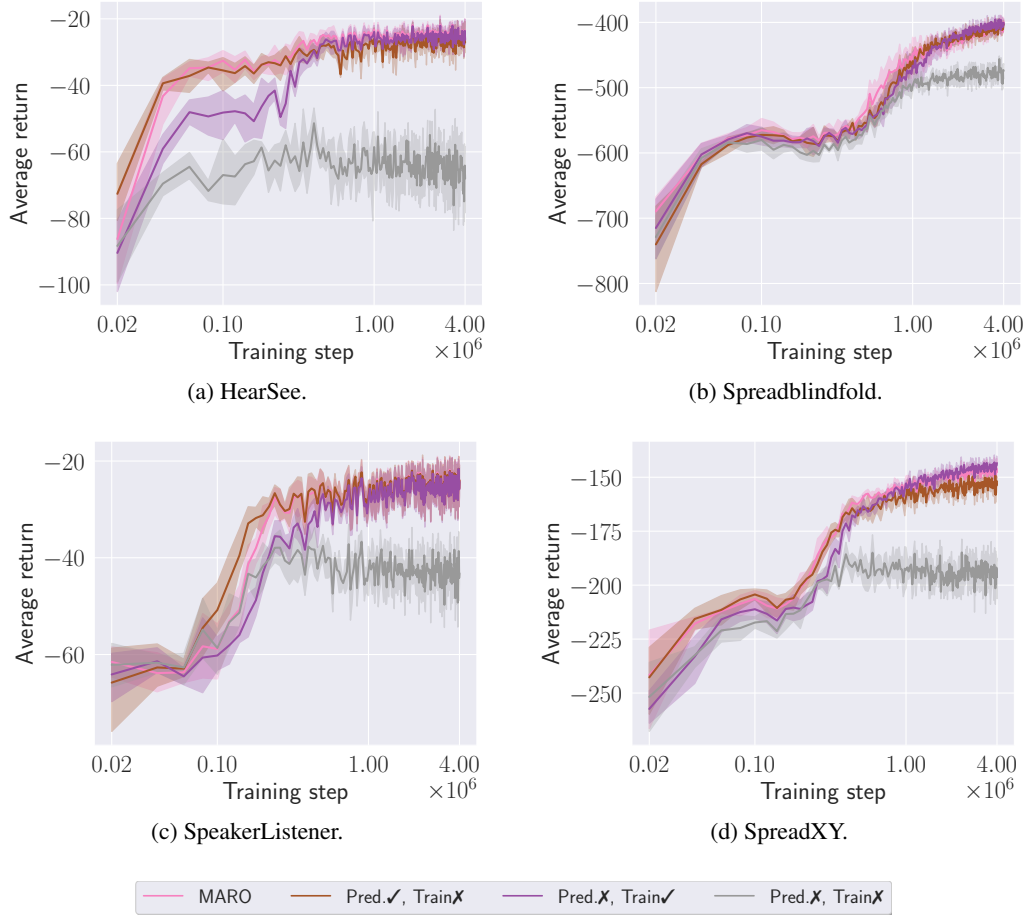


Figure 13: Average episodic returns during training with 95% bootstrapped confidence interval for $p \sim \mathcal{U}(0, 1)$, for MARO and the ablated versions across all environments, using the IQL algorithm.

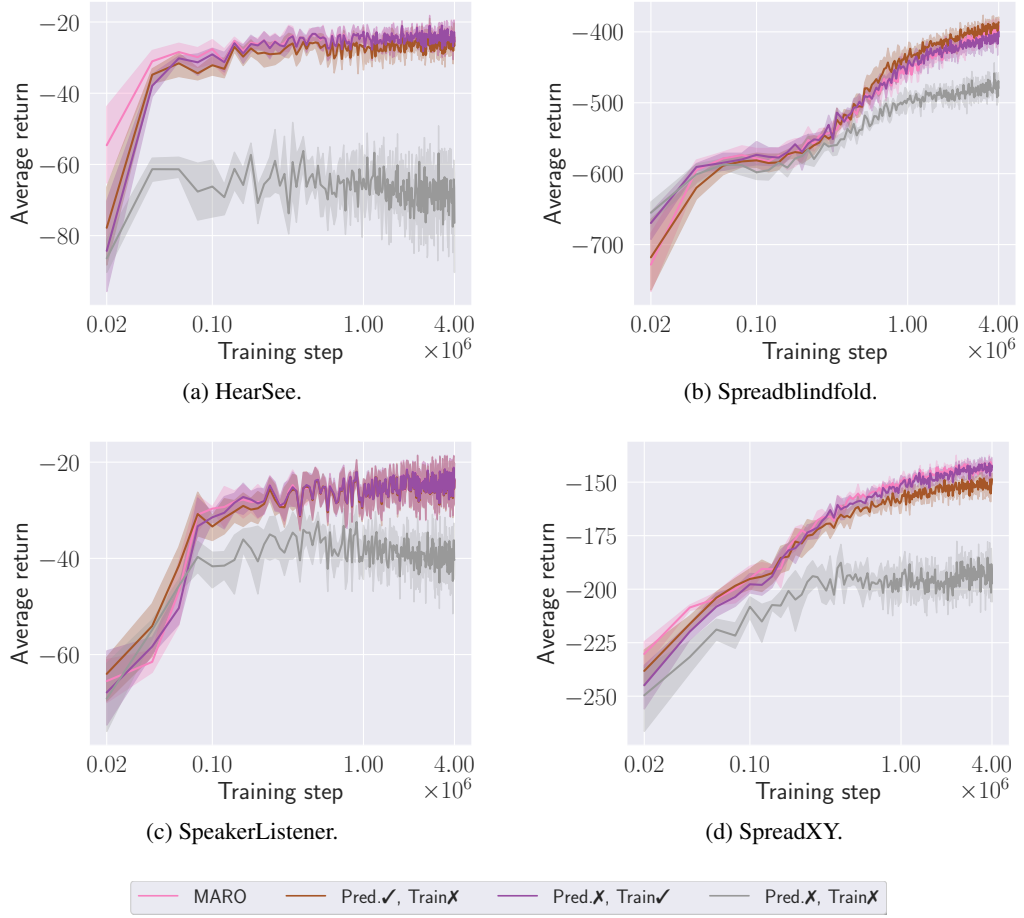


Figure 14: Average episodic returns during training with 95% bootstrapped confidence interval for $p \sim \mathcal{U}(0, 1)$, for MARO and the ablated versions across environments, using the QMIX algorithm.

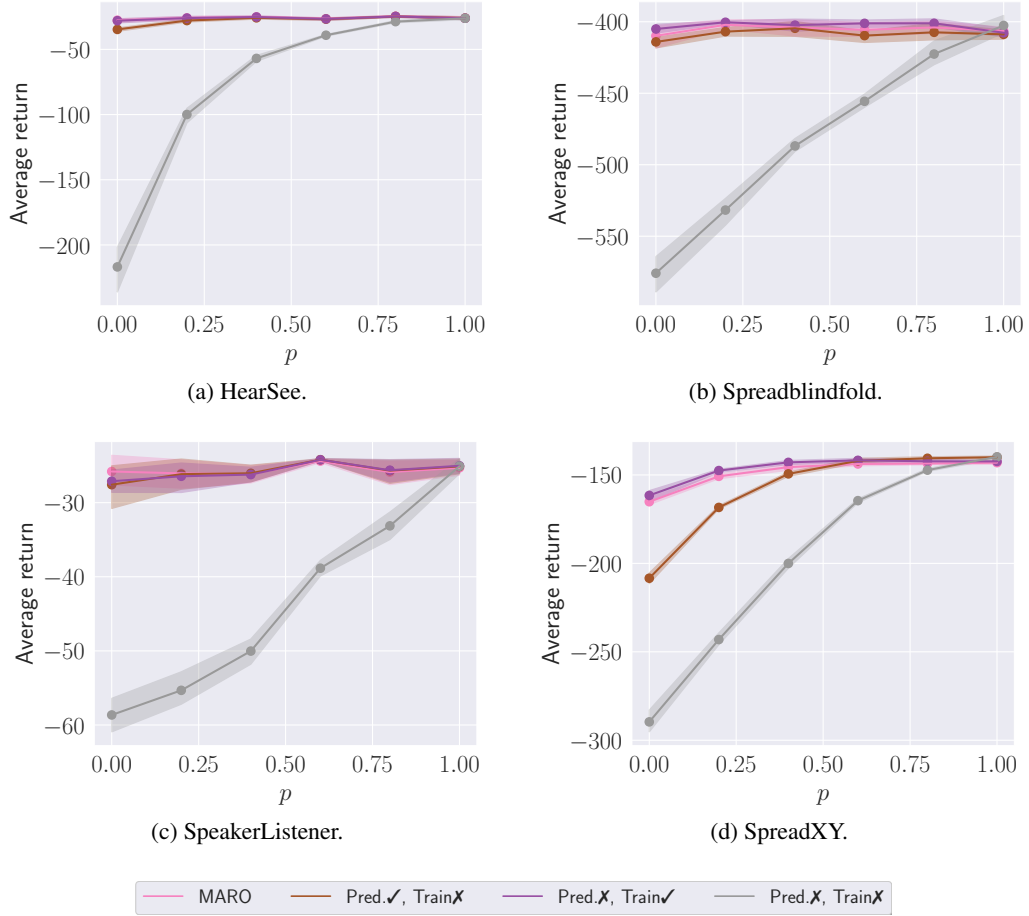


Figure 15: Average episodic returns with 95% bootstrapped confidence interval for different communication levels p at execution time, for MARO and the ablated versions across different environments, using the IQL algorithm.

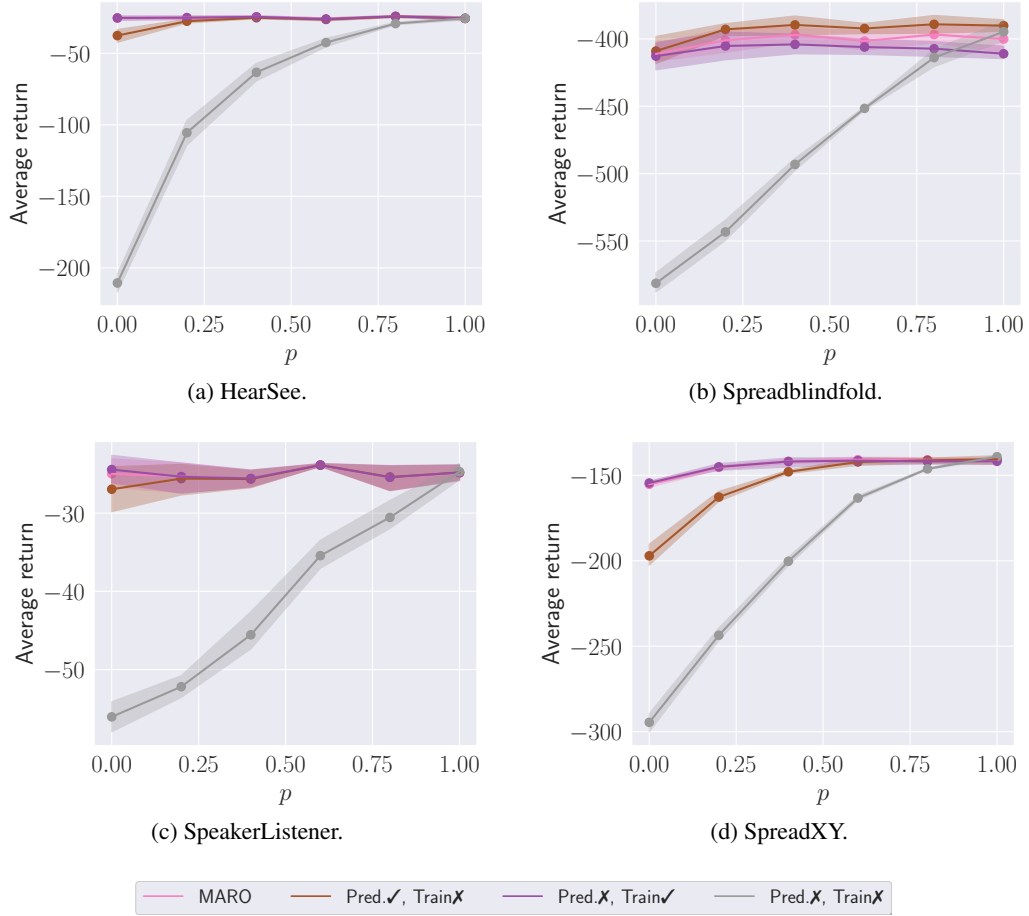


Figure 16: Average episodic returns with 95% bootstrapped confidence interval for different communication levels p at execution time, for MARO and the ablated versions across different environments, using the QMIX algorithm.

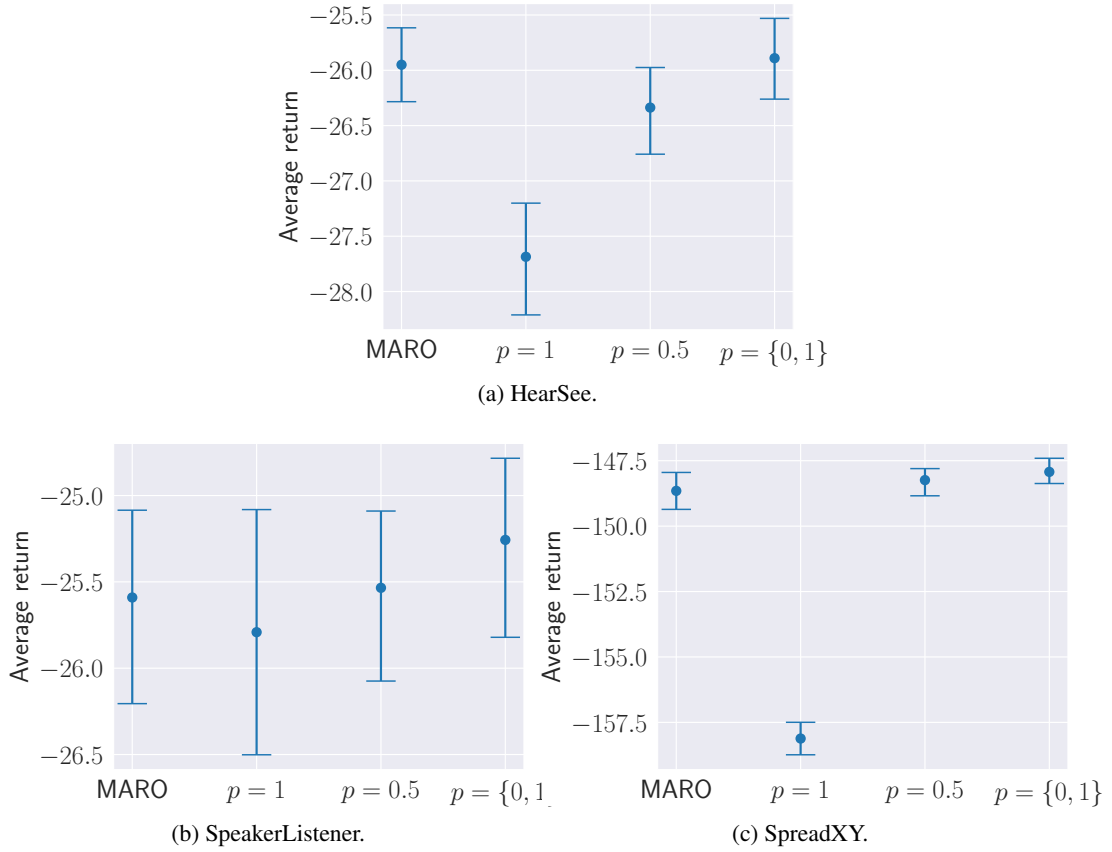


Figure 17: Average episodic returns at execution time with 95% bootstrapped confidence interval for $p \sim \mathcal{U}(0, 1)$, for different sampling methods of the training scheme of MARO across environments, using the IQL algorithm.

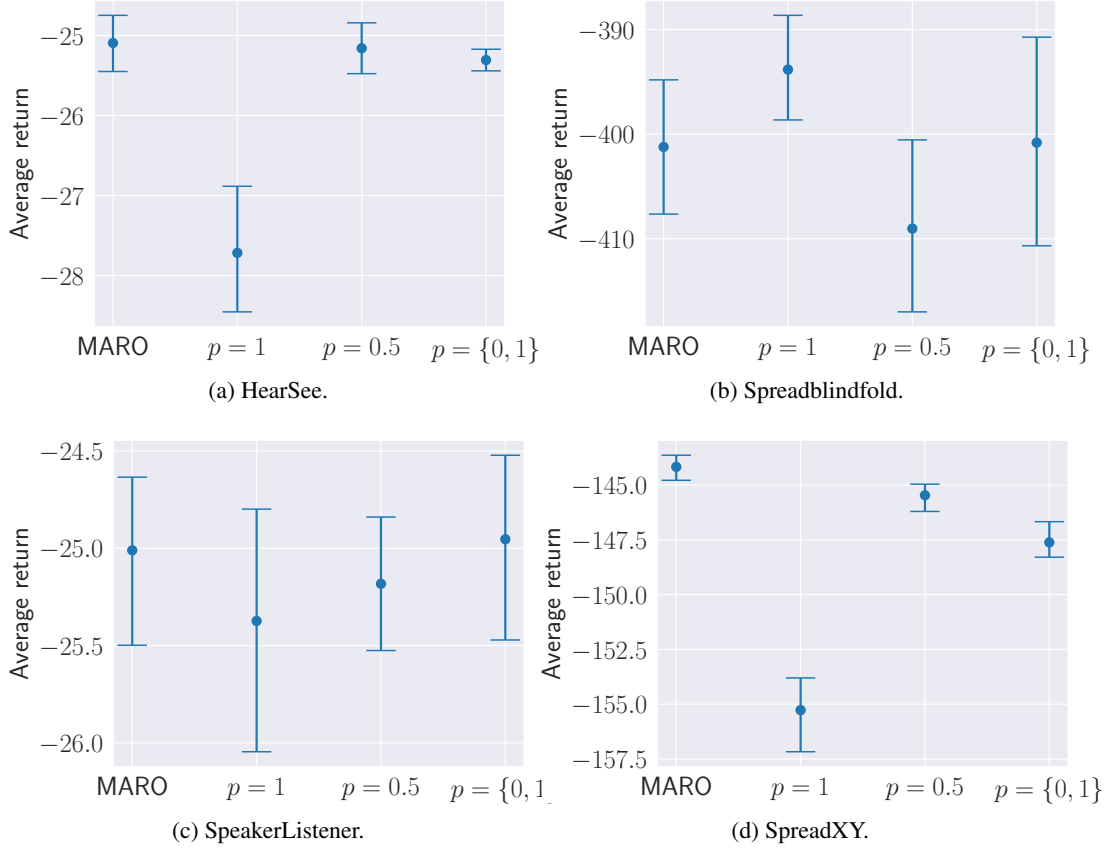


Figure 18: Average episodic returns at execution time with 95% bootstrapped confidence interval for $p \sim \mathcal{U}(0, 1)$, for different sampling methods of the training scheme of MARO across environments, using the QMIX algorithm.

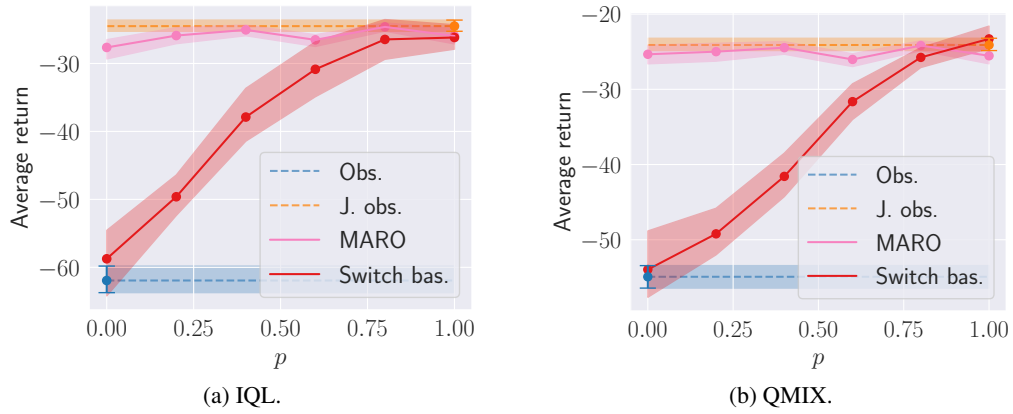


Figure 19: Average episodic returns with 95% bootstrapped confidence interval for different communication levels p at execution time for MARO and the Switch baseline in the HearSee environment.

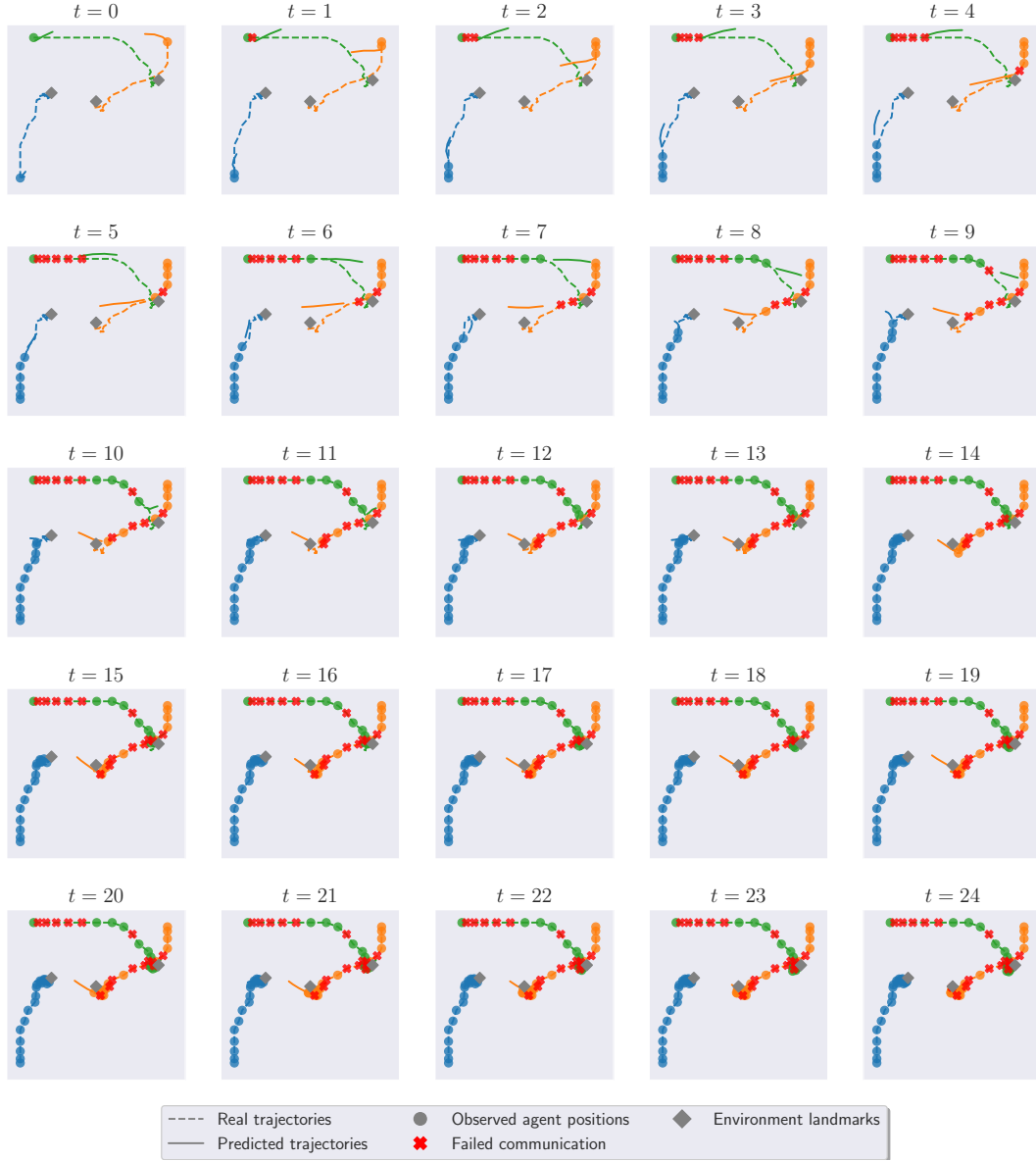


Figure 20: Trajectory prediction plots for the Spreadblindfold environment under the QMIX algorithm from the perspective of agent 0 (blue).

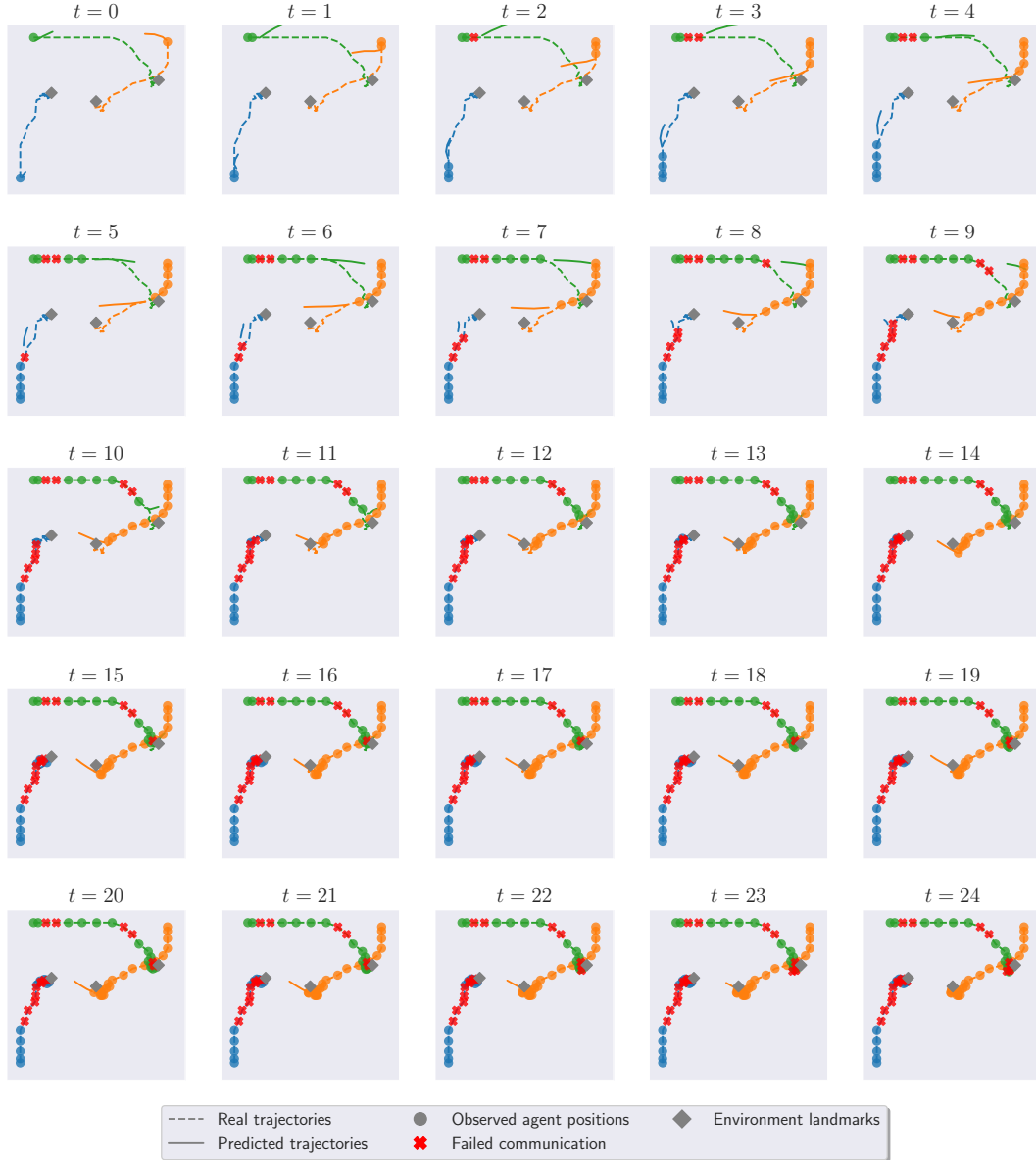


Figure 21: Trajectory prediction plots for the Spreadblindfold environment under the QMIX algorithm from the perspective of agent 1 (orange).

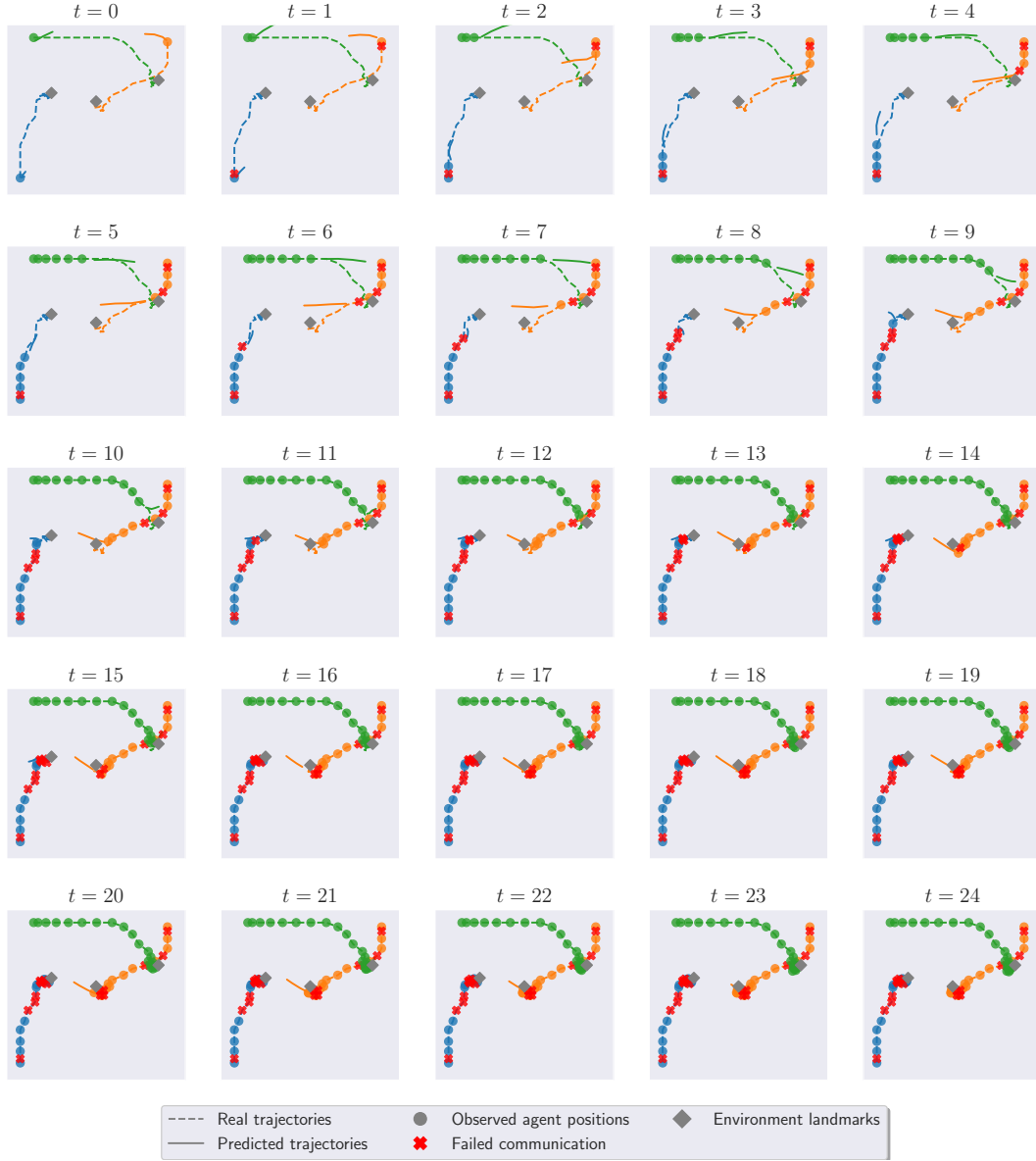


Figure 22: Trajectory prediction plots for the Spreadblindfold environment under the QMIX algorithm from the perspective of agent 2 (green).